AIMS Geosciences, 5(4): 831–867.
DOI: 10.3934/geosci.2019.4.831
Received: 18 April 2019
Accepted: 12 September 2019
Published: 30 September 2019

http://www.aimspress.com/journal/geosciences

Research article

The Tiller-Flotten research site: Geotechnical characterization of a very sensitive clay deposit

Jean-Sébastien L'Heureux[1,2,*], Anders Lindgård[1] and Arnfinn Emdal[2]

[1] Norwegian Geotechnical Institute (NGI), Trondheim, Norway
[2] Norwegian University of Science and Technology (NTNU), Trondheim, Norway

*** Correspondence:** Email: jsl@ngi.no; Tel: +4797120860.

Abstract: The Tiller-Flotten research site was developed through the Norwegian GeoTest site (NGTS) project. The site consists of a more than 50 m thick marine clay deposit. The top 7.5 m of the deposit shows a low to medium sensitivity, while sensitivity increases up to approximately 200 from 7.5 to 20 m below the ground surface. A wide variety of in situ and laboratory data have been acquired to investigate the geotechnical, geological and geophysical properties of the material. The sensitive clay shows low to medium plasticity and a liquidity index (I_L) above 1.6. It shows some overconsolidation (OCR ≈ 1.5–3.0) linked to the glacial history of the area. Its strength and stiffness properties show good agreement with some well-known correlations for sensitive clays. Anisotropy in undrained shear strength is also similar to other sensitive clays of Norway. It is hoped that the next years will see an increased use of this benchmark test site at Tiller-Flotten. The site can be used as a research tool, as training and teaching facilities and as ground for development of new soil models, testing of new investigation methods and further advance the state-of-the-art in sensitive clay material.

Keywords: sensitive clay; in situ test; laboratory test; geotechnical properties

1. Introduction

Deposits of sensitive marine clay are found over large areas of Norway, Sweden, Finland and Canada. Such deposits are extremely challenging to deal with for geotechnical engineers. In

particular, quick clay deposits are frequently associated with landslides triggered by natural or man-made events. Examples of such landslides in the Trondheim region are numerous, with well-known events at Rissa (1978) [1,2], Kattmarka (2009) [3] and Esp (2012) [4]. The challenges for geotechnical engineers working with sensitive clay material are often associated with sampling of undisturbed material, interpretation of in situ and laboratory data, and mapping the extent of the sensitive clay for landslide hazard assessment. There is thus a need to provide guidance to practicing engineers working in such problematic soils.

This paper focuses on the Tiller-Flotten geotechnical test site situated in Trondheim, mid Norway. The site was recently developed as a field research laboratory through the Norwegian GeoTest Site project (NGTS) [5]. It serves as a research tool, training and teaching facilities and as ground for development of new soil models, testing and calibration of soil investigation methods and further advance the state-of-the-art in sensitive clay material.

Despite the importance of these materials in Scandinavia and North America there are only few studies that report on the properties of sensitive and quick clay at an individual site e.g. [6,7]. The objective of this paper is to address this issue by presenting a detailed characterisation of the soils at Tiller-Flotten based on an integrated study including geotechnical, geological and geophysical data acquired both in the laboratory and in the field. The results presented herein form a useful reference to engineers working on sensitive soils. It is also hoped that the next years will see an increased use of the Tiller-Flotten benchmark site as a research tool.

2. Regional settings and site location

The Tiller-Flotten research site is situated approximately 10 km south of Trondheim in mid Norway (Figure 1). The site is primarily used for agricultural purposes and the area available for geotechnical studies is about 150 m by 300 m. Deposits at the site consist of marine and glaciomarine sediments that emerged from the sea following a fall in relative sea-level around the Trondheimsfjord region during the Holocene. The research site is at an elevation of 125 m.a.s.l. and drains towards the Nidelva river located at an elevation of 72 m.a.s.l. approximately 700 m to the southeast (Figure 2). In situ soundings reveal the total sediment thickness at the site is above 50 m.

The area surrounding the site is also characterized by thick deposits of marine clay with ravines and landslide scars omnipresent (Figure 2). The devastating 1816 Tiller landslide that led to 15 casualties is located at only a few hundred meters from the research site [8]. A close look at the LIDAR imagery from the area likely shows traces of a pre-historic landslide scar to the northeast of the geotechnical research site (Figure 2). On Figure 2 the location of other well characterised quick clay sites in the vicinity is also shown, namely Tiller [6] and Klett [9]. The location of the NGTS sand research site at Øysand [10] is also indicated.

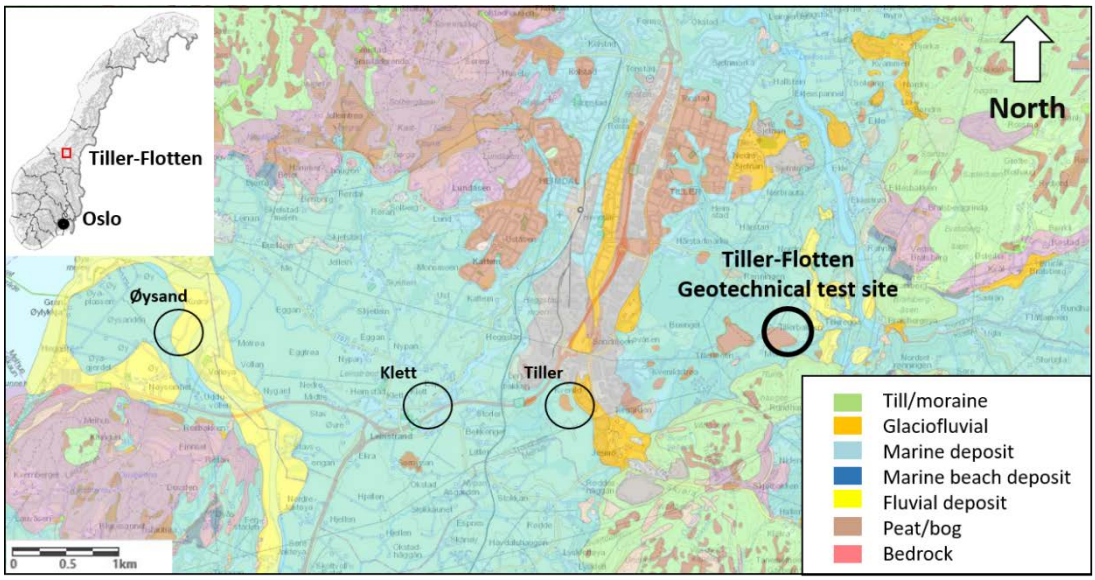

Figure 1. Quaternary geology surrounding the Tiller-Flotten Geotechnical test site in Trondheim.

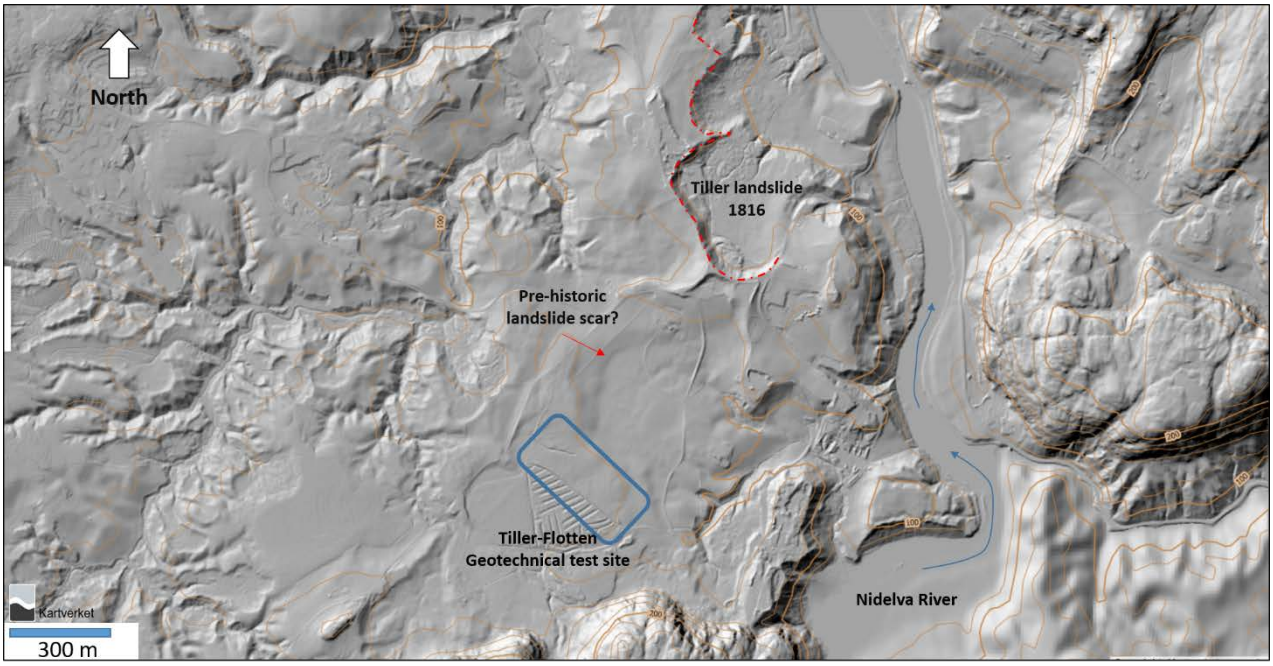

Figure 2. LIDAR data for Tiller-Flotten area (data from www.hoydedata.no). The blue square marks the limits of the Tiller-Flotten Geotechnical test site. Blue arrows show the direction of river flow.

3. Field and laboratory data

Site characterization at Tiller-Flotten started in 2016 as a part of the Norwegian GeoTest Sites project [5,11]. A wide range of in situ tools, geophysical techniques, sampling techniques and

laboratory tests have been used to assess the geological history and geotechnical properties of this sensitive clay deposit. A complete overview of in situ tests, sampling methods and geophysical tests performed at the site is given in Table 1. Table 2 presents a list of laboratory tests performed on the samples retrieved from the site. The reader is referred to NGI [12,13] for more information on the testing methods and standards followed. Most of the tests were performed in the southern part of the study area with a minimum spacing of 2 m between the boreholes or in situ soundings. Several tests were also conducted around the perimeter of the study area and the results are consistent with those found in the southern corner.

Table 1. Summary of in situ tests, sampling methods used and geophysical tests performed at the Tiller-Flotten research site.

	Testing methods in the field	Abbreviation
In situ tests	Cone penetrometer also with resistivity and seismic modules	CPTU, RCPTU, SCPTU
	Dilatometer and Seismic dilatometer	DMT, SDMT
	Push-in-pressure cells	–
	Piezometers	P
	Field vane test	FV
	Rotary pressure soundings	RP
Sampling	Geonor (ϕ 72 mm) fixed piston	–
	Geonor (ϕ 54 mm) fixed piston (composite)	–
	Sherbrooke block (ϕ 250 mm)	–
	Mini-block (ϕ 160 mm) [14]	–
Geophysics	Multiple analysis of surface waves	MASW
	Electrical resistivity tomography	ERT

Table 2. Summary of laboratory tests performed on samples from Tiller-Flotten.

Testing methods in the laboratory	
Water content analysis (WC)	Multi sensor core logging (MSCL) including gamma density and magnetic susceptibility (MS)
Unit weight (density)	Split core imaging
Unit weight of solid particles	Oedometer tests at constant rate of strain (CRS)
Atterberg limits	Hydraulic conductivity
Grain size distribution (GSD)	Triaxial - Anisotropically consolidated undrained compression tests (CAUC)
Fall cone test (FC)	Triaxial - Anisotropically consolidated undrained extension tests (CAUE)
Salinity	Direct simple shear (DSS)
X-ray diffraction (XRD)	Bender element test
X-ray inspection (XRI)	Scanning Electron Microscopy (SEM)
Unconfined compression tests (UC)	

4. Engineering geology

4.1. Depositional environment

Retreat of the glaciers in the Tiller area occurred about 12,000–11,000 years ago [15]. The warmer climate during that period led to a rapid retreat of the glaciers in the valleys and rapid accumulation of glaciomarine materials (mostly clay) in the fjords. This phase likely included rapid suspension settling, strong bottom current and deposition of ice rafted debris from icebergs (IRD). At around 11,000 years ago, the climate deteriorated in Northern Europe leading to a re-advance of the glaciers with its peak at around 10,600 years ago [16,17].

Approximately 10,500 years ago, a short and warmer climate period led to glacial melting in the study area [16]. This development was rapidly interrupted by a new cold period that reached its maximum at 10,300 years ago. The glaciers were then steady for a longer time period leading to the deposition of lateral and frontal moraines close to the research site. The climate improved following this period and the glaciers retreated towards the east in the valley.

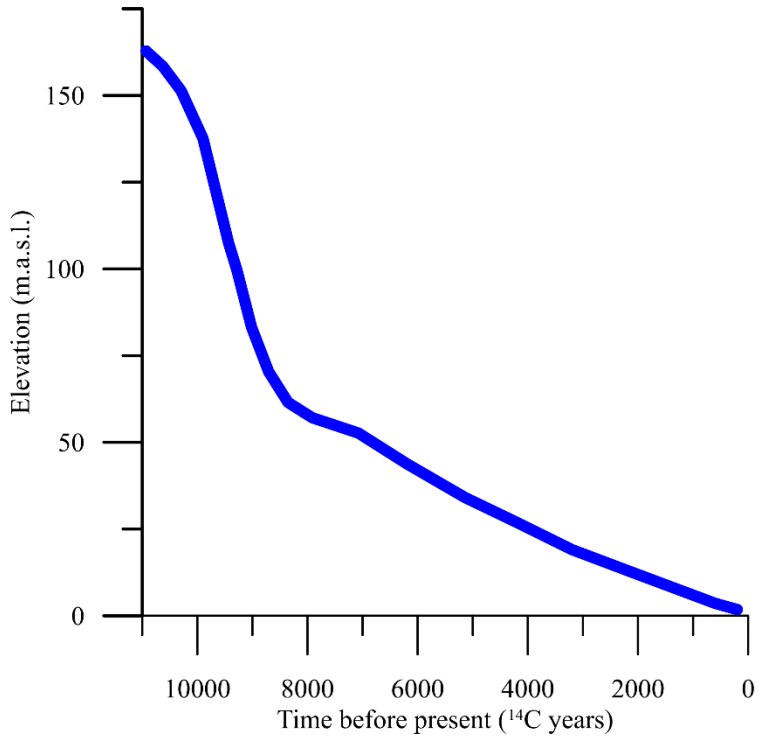

Figure 3. Shoreline regression curve for Trondheim, adapted from [8].

The removal of the ice weight led to a readjustment of the crust (glacio-isostatic uplift) in the Holocene period. This led to a relative fall of sea-level and to the emergence of the seabed (marine regression). The marine limit in Trondheim is at 175 m above present day sea-level. The high rate of glacial isostatic adjustment in the early Holocene phase led to rapid deposition of glaciomarine and marine clays. Based on the shoreline regression curve for the Trondheim region, it is expected that deposition at the study site took place in a fjord environment (saline environment) at a maximum

water depth of 30–40 m (Figure 3). These conditions progressively changed towards estuarine conditions and beach conditions as the relative sea-level felt and the site emerged from the sea some 9500 years ago.

4.2. Source of material

The bedrock in the Trondheim region was formed about 500 million years ago [18]. It is dominated by volcanic rocks such as greenstones and tuff. These metamorphosed and moved into place during the Caledonian orogenesis. There are also local outcrops consisting of meta-sedimentary such as sandstone and shales. Most of the clay material that deposited in the fjord derived directly from glacial erosion of the bedrock, but also from erosion of glacial deposits in the Holocene. The major mineralogical components of the bedrock and glacial deposits in the catchment are quartz, feldspars, illite and chlorite with the latter making up the main proportion of the clay fraction.

4.3. Post depositional processes and timing

As the clay deposit emerged from the sea it was exposed to leaching from fresh groundwater flow. Fresh water percolating downwards through the marine deposits removed the salt ions and left behind a metastable, sensitive structure made up of flocculated clay minerals. The high sensitivity of Norwegian quick clays is usually attributed to the leaching by fresh groundwater of the salts within the grain structure [19].

During its emergence the clay deposit was covered by coarse beach and fluvial deposits. However, most of the coarse sediment was removed in historical time and used as an aggregate in various construction projects. The thickness of this deposit is unknown, but may have been to 2–3 m.

Once above sea level sub aerial exposure has produced a weathered crust. This crust is close to the soil surface and, through weathering, drying and cracking, has changed its properties and become firm.

4.4. Stress history

Groundwater level at the site is presently located 1 m to 2 m below ground level. Numerous piezometers were installed in 2017 to monitor changes in pore-water pressure over time at the site. Results are shown in Figures 4 and 5. The groundwater pressure is below hydrostatic conditions and show a nearly linear increase with depth between 5 m to 23 m below ground level (Figure 4). It is thought that the downward gradient observed is caused by drainage to the east due to the regional groundwater flow in the area and the large differences in ground elevation.

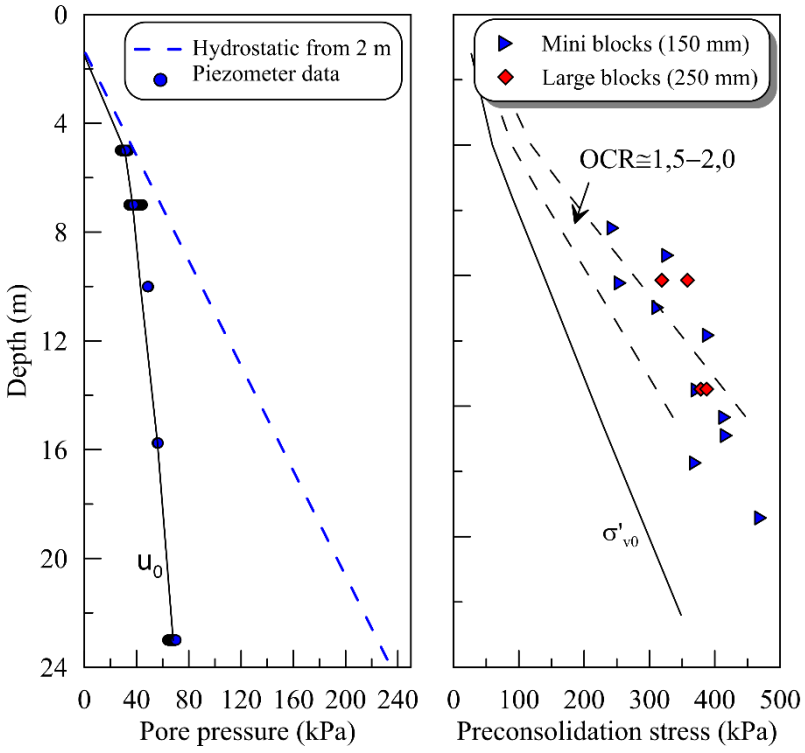

Figure 4. In situ piezometric profile (u_0), effective stress profile (σ'_{v0}) and preconsolidation stresses (σ_p') from 1D oedometer testing on block samples.

Preconsolidation stress (σ_p') was estimated from constant rate of strain (CRS) oedometer tests on high quality Sherbrooke block samples and mini block samples. Values of σ_p' were obtained using the Karlsrud and Hernandez-Martinez method. This method simply takes the pre-consolidation pressure as the average stress between where the tangent modulus starts to drop off and until it starts to climb up again along the virgin modulus line.

The results for oedometer tests on the mini-block samples are shown on Figure 4. All of the values are above the in situ vertical effective stress (σ_{v0}') line throughout the profile. The estimated σ_p' values lead to overconsolidation ratio (i.e. OCR = σ_p'/σ_{v0}') above 2 in the first 10 m below ground level, and between 1.5–2.0 from 10 m and below. The clay at the Tiller-Flotten site likely deposited in a shallow marine and brackish environment with little or no topographic relief and gentle slopes. Some loading events might have occurred as a result of the glacier re-advance during and prior to the Younger Dryas period, and this may explain some of the apparent pre-consolidation observed in the clay (Figure 4). Subsequent emergence of the region during the Holocene lead to the erosion of neighboring slopes and to the development of the Nidelva river valley to the east. Valley formation likely have, with time, contributed to a change in groundwater flow at the site and consequently changes in stress in the clay deposit. The apparent pre-consolidation may also, in part, be attributed to secondary consolidation or creep in the clay deposit [20], and to chemical changes as suggested by Bjerrum [21].

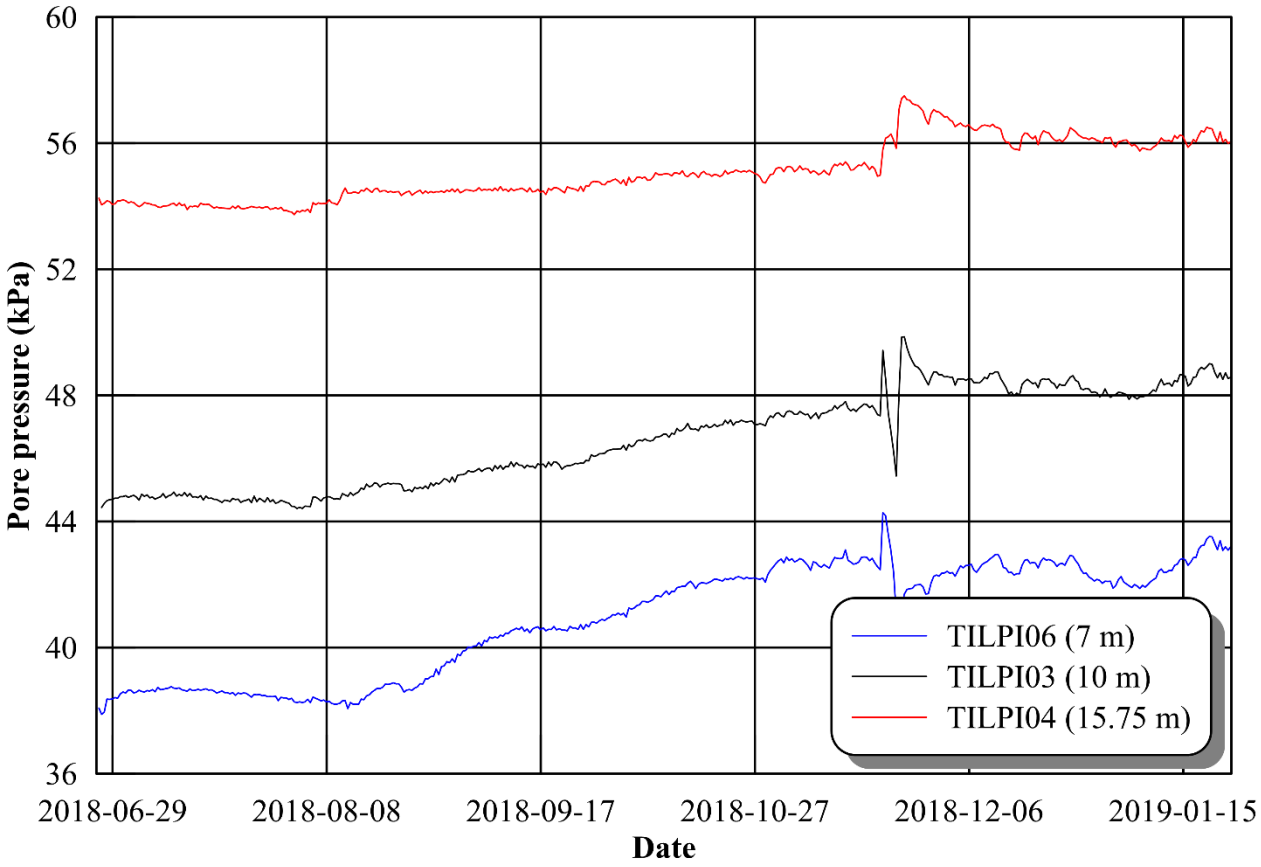

Figure 5. Pore water pressure data at Tiller-Flotten with time for piezometer located at 7 m, 10 m and 15.75 m below the surface.

4.5. Temperature

Ground temperature data were registered at several occasion at the Tiller-Flotten research site by means of temperature sensors installed within CPTU penetrometers. The sensors have a precision of +/− 0.5 °C and show a relative constant temperature of 4 °C below a depth of 6 m (Figure 6). Such measurements should be reliable in sensitive clay as the impact of frictional heat when pressing the CPTU rod is assumed to be low. Piezometers with temperature logging show similar temperature values.

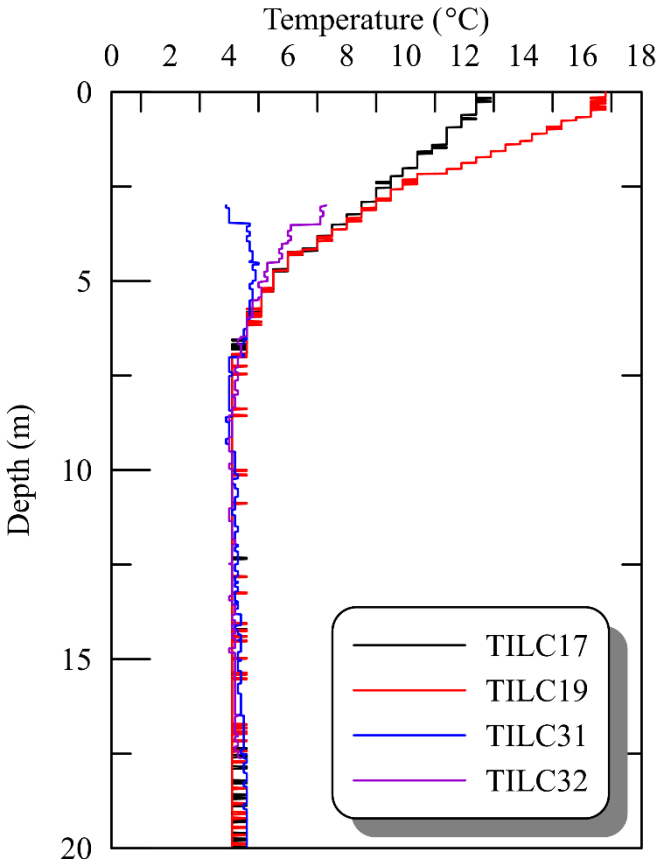

Figure 6. In situ temperature data collected by means of CPTU.

4.6. Stratigraphy

The stratigraphy at the site is divided into two main units based on laboratory and in situ testing results (Figure 7). The top unit (Unit I) is ca. 2 m thick and consists mostly of desiccated and weathered clay. Unit II is divided in two parts (i.e. Unit IIA and IIB). Both sub-units show similar clay content and structure but differ in terms of soil sensitivity. The clay of Unit IIA is found from 2 to 7.5 m below the surface and shows a low to medium sensitivity. From 7.5 m below the ground surface the clay shows extreme sensitivity, often above 100.

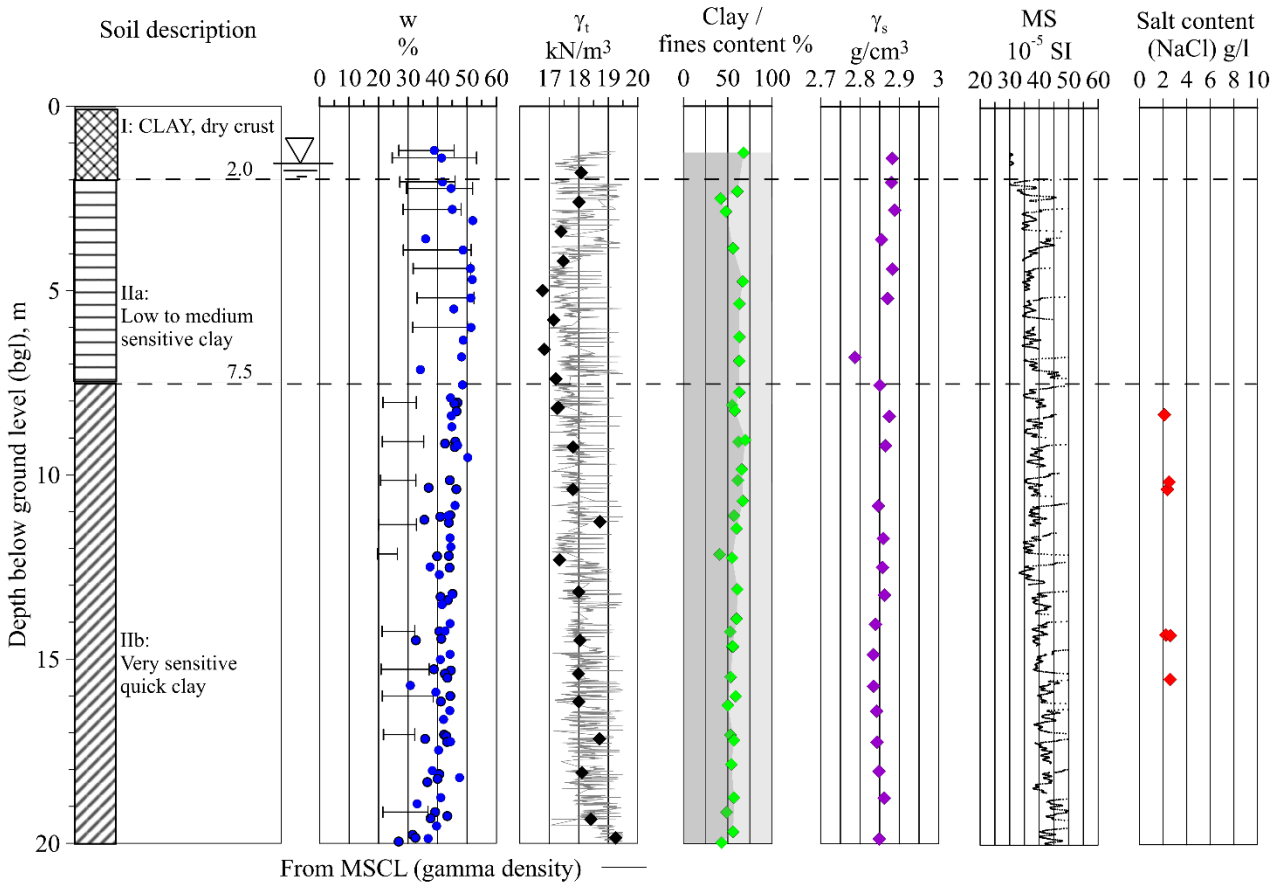

Figure 7. Basic soil profile, stratigraphy and index properties at the Tiller-Flotten site. w = water content, γ_t = bulk unit weight, γ_s = particle density, MS = magnetic susceptibility.

4.7. Structure and fabric

X-ray analyses show that the clay of Unit II is laminated with darker and lighter intervals (Figure 8). These light and dark coloured couplets are also observed in split core sections and are interpreted as varves (Figure 9). The varves are found throughout the whole core section down to a depth of 20 m below the ground surface. Such varves likely formed in the marine/brackish environment from seasonal variation in clastic, biological and sedimentary processes. The light layer usually comprises a coarser sediment with input of silt and thin sand layers deposited under higher energy conditions. On the inverse, the dark layer likely deposited during winter months, when meltwater and associated suspended sediment input was reduced, and often when the lake/fjord surface was frozen. In addition to seasonal variation of sedimentary processes and deposition, varve formation requires the absence of bioturbation. Consequently, these varves may have formed under anoxic conditions.

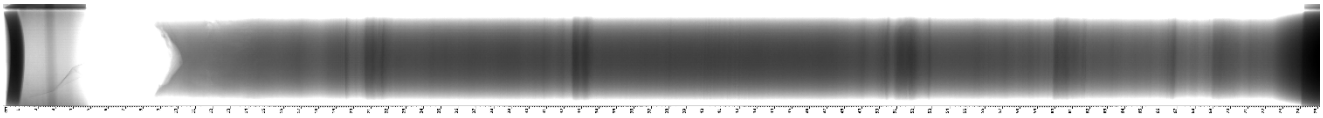

Figure 8. Example of X-ray image from a 54 mm sample showing light and dark coloured couplets in Unit II.

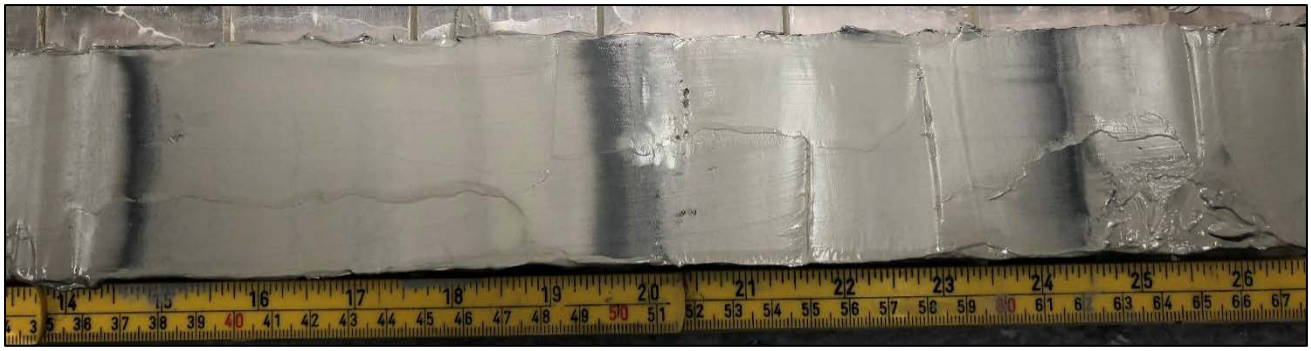

Figure 9. Picture of split core section showing typical light and dark colored couplets interpreted as varves in Unit II at Tiller-Flotten.

4.8. Grain size distribution

The log of Figure 7 presents clay size particle content and fines content with depth. Results were determined using hydrometer method (ISO 17892-4:2016). The clay content ranges from 45–70% and seems to decrease a little with depth, from 70% at 7.5 m to a value of 50% at 19 m. Grain size distribution analyses were also performed using the falling drop method [22] and the results compare well with those obtained through hydrometer analysis (Figure 10). According to NGF (2011) [23], as the material has a clay content greater than 30%, it should be classified as a clay.

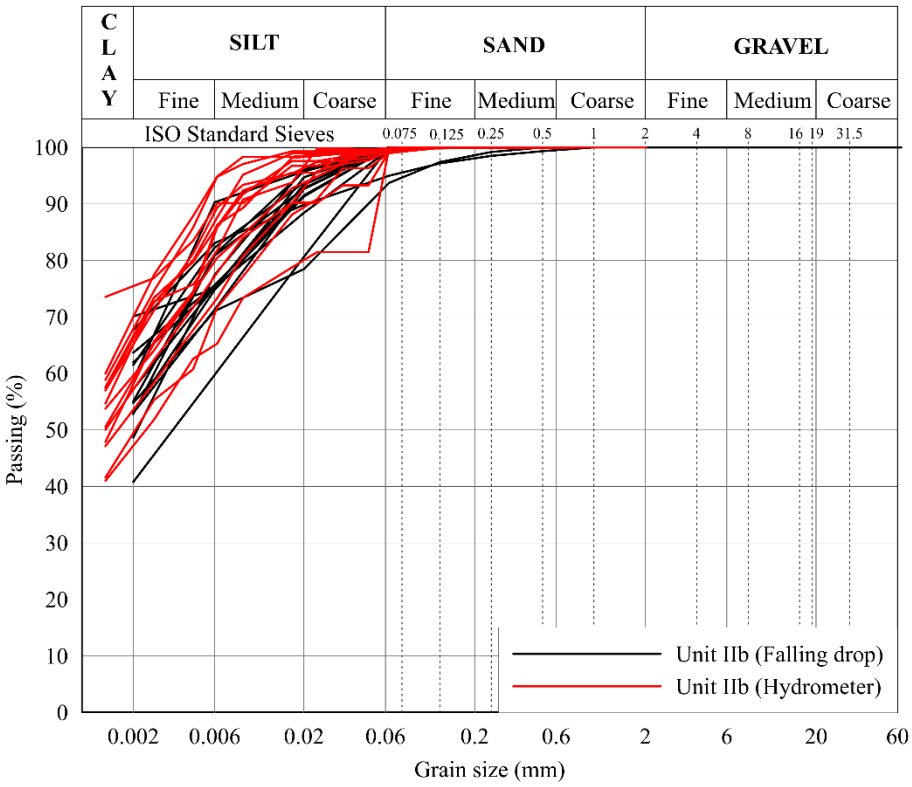

Figure 10. Results from grain size analysis using the hydrometer and falling drop methods.

4.9. Particle density

Particle density values (G) for Tiller-Flotten clay were determine using the fluid pycnometer method. Two tests were performed on each specimen. Except for an outlier at 6.8 m below ground level, results show that all test data fall within a narrow range of 2.83 to 2.88 g/cm^3 with an average of about 2.85 g/cm^3 (Figure 7). These are typical values for Norwegian clays.

4.10. Pore water chemistry

Salt content values for the pore fluid were measured on samples from 8 and 15 m below the ground surface. Values are low and showed salt contents (NaCl) of 2.1 g/l and 2.6 g/l at both depth, respectively. These data suggest that the material has been leached post deposition over the entire studied thickness.

5. State and index properties

5.1. Water content

The plot of basic index parameters shown in Figure 7 confirms the fairly high degree of uniformity at the Tiller-Flotten site. Natural water content slightly increases from a value of 40% close to the surface to a value of 50% at a depth of 5 m; before decreasing to about 30–35% at 20 m

depth. Except for the crust, the degree of saturation of the clay is expected to be at 100%. The natural water content is below the liquid limit w_L throughout Unit IIA, while it is higher than w_L in Unit IIB.

5.2. Bulk or total unit weight

Measured bulk density values for the Tiller-Flotten clay are presented on Figure 7. The total unit weight of the clay shows a trend inverse to that of the water content profile with a slight decrease from a value of 18 kN/m^3 close to the surface to a value of 16.8 kN/m^3 at a depth of 5 m; before increasing to about 19 kN/m^3 at 20 m depth. Results from multisensor core logger show changes in bulk density throughout the soil column that is likely linked to the varved layers. The overall average value of bulk density is about 18.0 kN/m^3.

5.3. Atterberg limits

Plasticity index (Ip) is plotted against depth on Figure 7. The overall trend is for the values to fall from about 20% in Unit IIA to values in the range 8–15% in the very sensitive quick clay of Unit IIB. On the plasticity chart the low to medium sensitive clay of Unit IIA plots just below the A-line and corresponds to a clay of medium plasticity, while the sensitive clay of Unit IIB plots in the CL zone of low plasticity (Figure 11). This classification is consistent with that from the particle size distribution curves presented above.

Liquidity index (I_L) is a very useful parameter for assessing the structure and stress history of a clay deposit. It has been shown to correlate well with compressibility, strength and sensitivity properties of fine grained materials [24]. It is defined as:

$$I_L = \frac{w - w_p}{I_p} \tag{1}$$

where : w_p is the plastic limit.

If the water content equals the liquid limit (w_L) the liquidity index will equal 1. According to Leroueil et al. [25], if the water content exceeds the w_L, the relationship between I_L and remoulded shear strength (s_{ur}) can be expressed as follow:

$$s_{ur} = \frac{1}{(I_L - 0.21)^2} \tag{2}$$

If I_L exceeds about 1.6, this expression suggests that s_{ur} will be less than 0.5 kPa suggesting that the material will be very sensitive or even quick. Data from Tiller-Flotten, shown on Figure 12 show the value to increase with depth from about 1 in the upper, low to medium sensitive clay unit IIa, to values up to 9.3 in the lower clay unit (IIb). Overall the values are very high suggesting the material to be very sensitive. These I_L values suggest that the material possesses a high degree of structure and is consistent with that which has been deposited slowly in still water leading to an open random fabric [26]. The I_L data shown on Figure 12 also seem to be affected by sample quality. Indeed, values obtained from 54 mm piston sample are generally higher than those obtained from high quality piston samples.

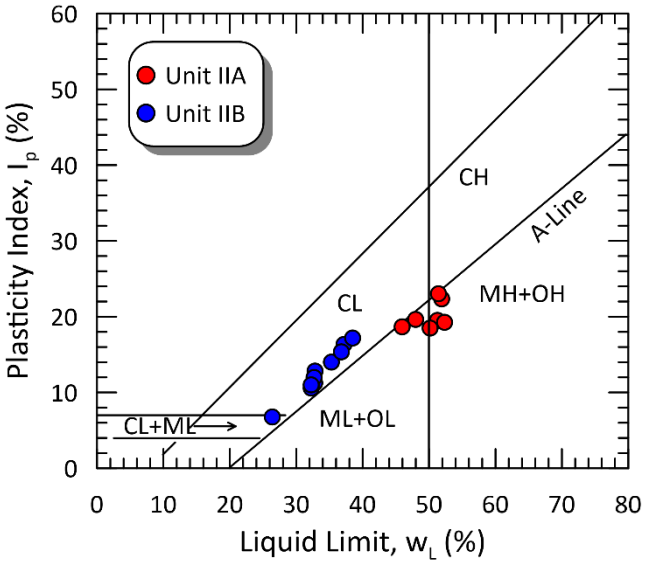

Figure 11. Plasticity chart for the Tiller-Flotten clay.

5.4. Sensitivity and remoulded undrained shear strength

The Tiller-Flotten clay is expected to have a high degree of sensitivity due to its depositional history which lead to a flocculated and open material structure, and to post-depositional processes that leached the salt content of the pore water. The sensitivity (S_t) of a geo-material is defined as the ratio of the intact undrained shear strength (s_u) to the remoulded undrained shear strength (s_{ur}). According to NGF [23] a clay material is defined as "very sensitive" if S_t values are greater than 30. Furthermore, a clay in Norway is defined as quick if the s_{ur} is less than 0.5 kPa.

Results from fall cone data showing sensitivity and remoulded undrained shear strength for the Tiller-Flotten clay are presented on Figure 12. The data shows that the clay is not sensitive down to 7.5 m below the ground level. Beyond this depth the remoulded strength falls below 0.5 kPa and the sensitivity of the clay is high.

Strength sensitivity can vary depending on sample quality and on the technique used to measure it. As seen on Figure 12 there is large scatter in the sensitivity data when comparing results obtained from block samples and from 54 mm piston samples. This is linked to sample quality being lower for 54 mm samples and hence lower peak undrained shear strength is measured on these samples. From 4 m below the ground surface, in situ vane tests were performed at Tiller-Flotten. Results show higher s_{ur} than that obtained on the samples tested in the laboratory. As shown later in this paper the intact undrained shear strength is also lower than that measured in the laboratory hence leading to a lower sensitivity. The somewhat contrasting values obtained with the in situ vane are linked to aspects of strain localization and excess pore pressure generation. This has been discussed by several authors (e.g. [27]).

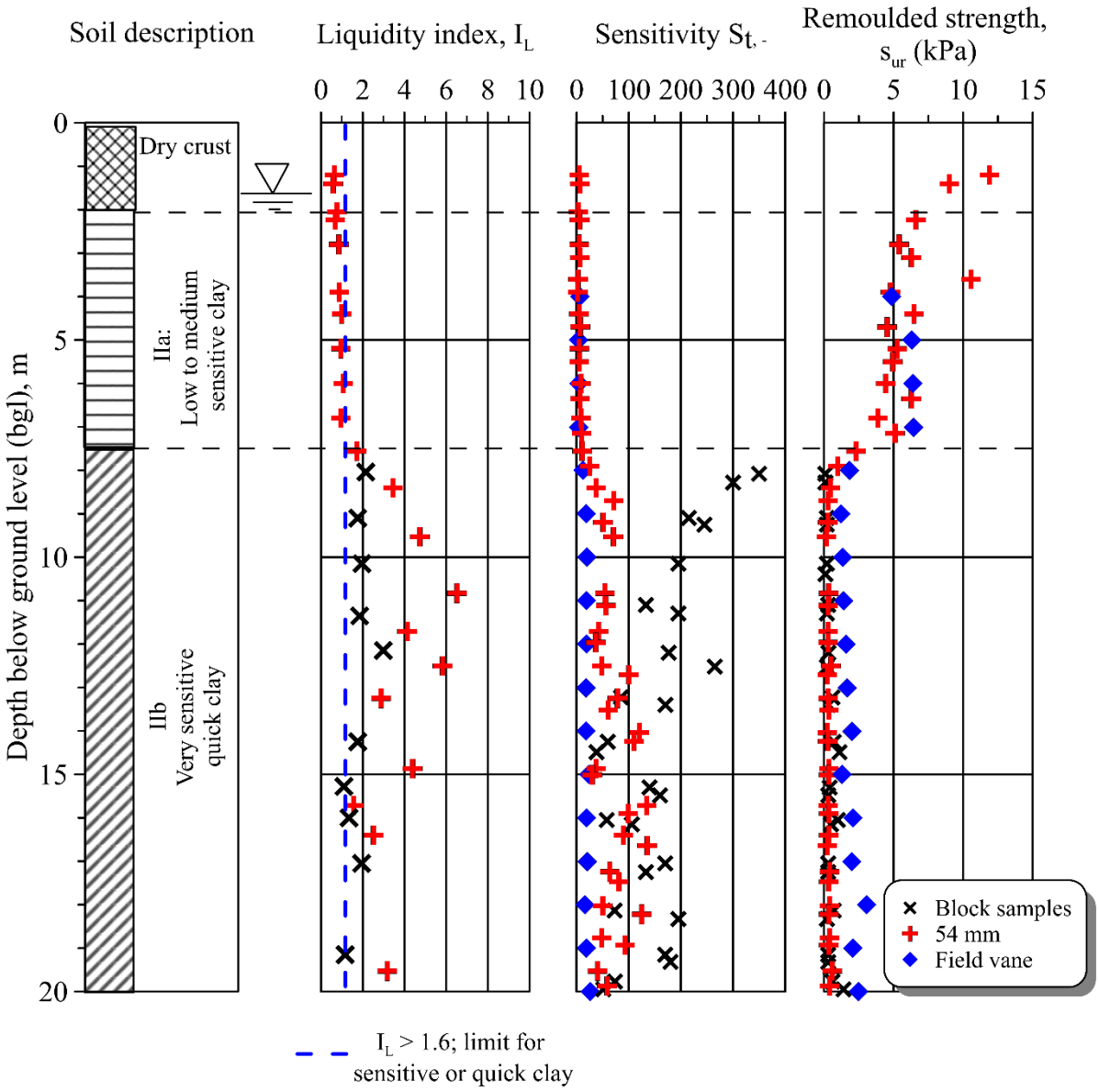

Figure 12. Plot of liquidity index, sensitivity and remoulded strength with depth.

5.5. Identification of quick clay from rotary pressure soundings

In practice, distinguishing between quick and non-quick clays is a major challenge for geotechnical engineers, especially in Scandinavia. The rotary pressure sounding tool is traditionally used in Norway to delineate quick clay pockets in early project stages. Plots are made of the penetration resistance versus depth and the zones over which the penetration resistance remains constant or decreases with depth are considered to be likely quick clay zones. For full details of the methods the reader is referred to NGF [28].

Some examples of rotary pressure sounding data across the whole Tiller-Flotten study site are shown on Figure 13. The method works well to delineate the quick clay unit at this site. The data is fairly homogenous throughout the whole site area.

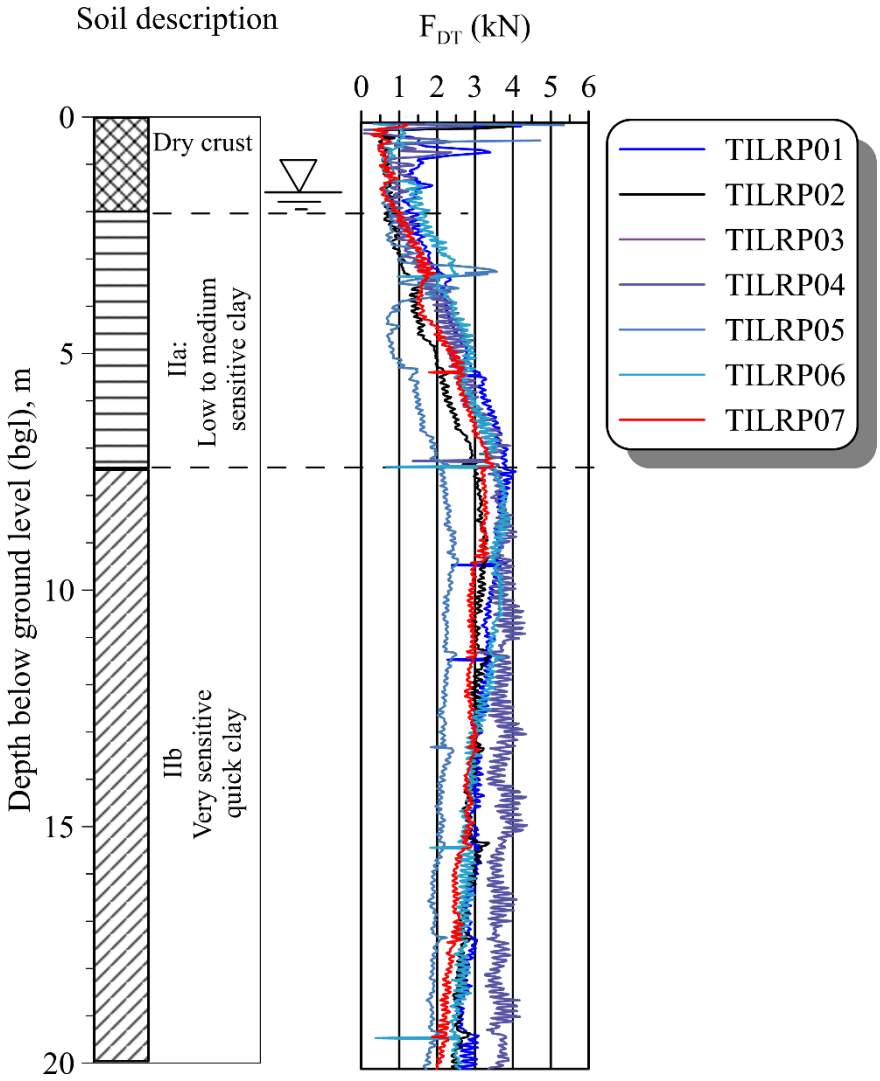

Figure 13. Results from selected rotary pressure soundings at Tiller-Flotten.

5.6. Identification of quick clay from CPTU tests

An alternative approach to identifying the presence of sensitive and quick clay in practice is to make use of the piezocone data (CPTU). Typical CPTU results for the Tiller-Flotten clay are presented in Figure 14. The data is presented in the form of corrected tip resistance (q_t), sleeve friction (f_s) and pore pressure generated behind the tip of the cone (u_2). The data from four typical CPTU tests at Tiller-Flotten are fairly consistent. However, it is not evident from this data only (i.e. q_t, f_s and u_2) to distinguish between low sensitive and very sensitive clay, though there appears to be a reduction in the f_s values to their minimum values at the top of the sensitive clay. A similar pattern has been observed in the Klett clay [9].

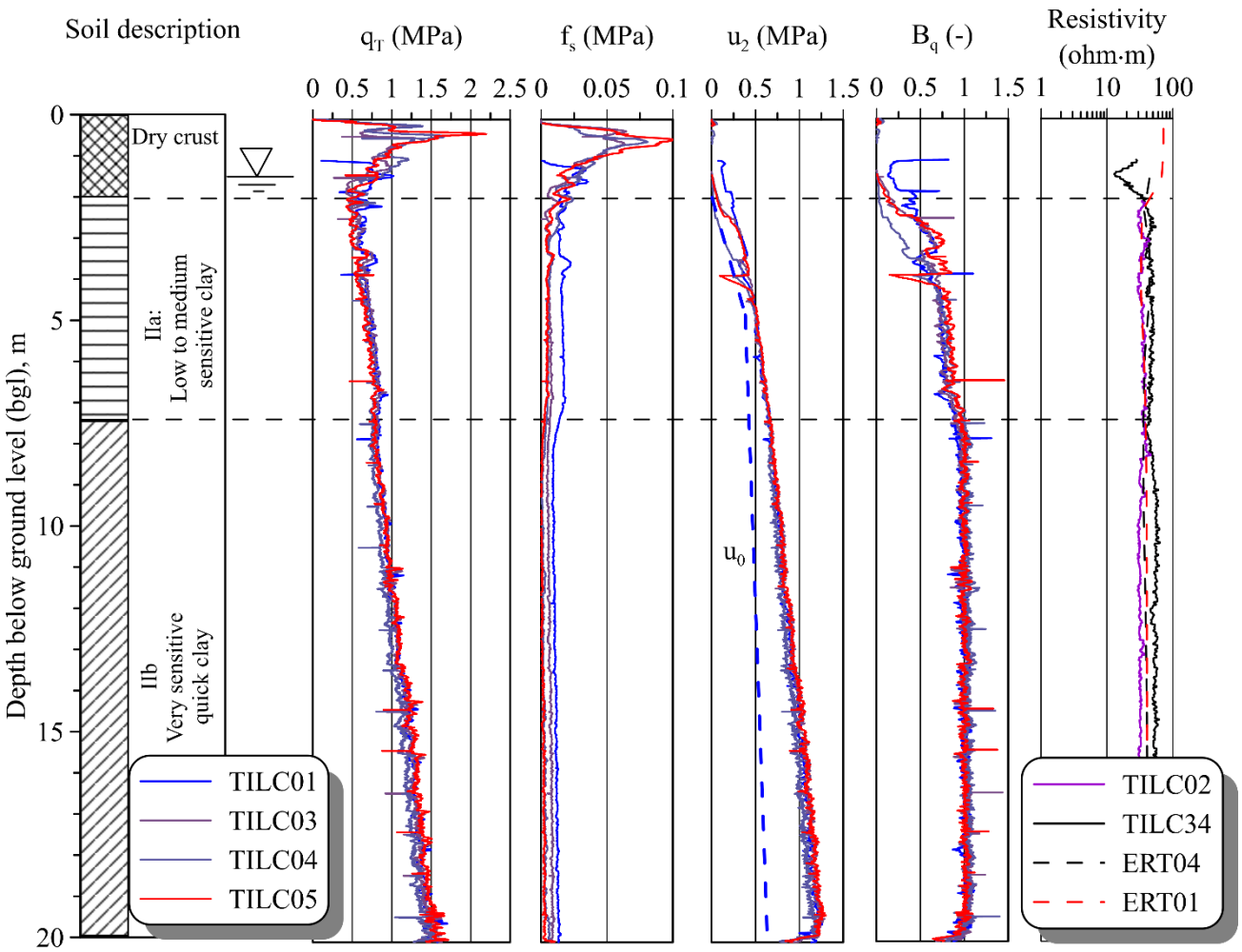

Figure 14. Typical CPTU and RCPTU test results for Tiller-Flotten showing corrected tip resistance q_t, sleeve friction f_s, pore-pressure during penetration u_2, pore pressure parameter B_q, and electrical resistivity ρ.

Previous researchers have shown that there is a strong possibility of having a quick material when the normalized pore water pressure parameter B_q exceeds 1.0 [29]. The pore pressure parameter is defined as:

$$B_q = \frac{q_t - \sigma_{v0}}{u_2 - u_0} \quad (3)$$

where σ_{v0} is the total overburden stress. Results from CPTU data at Tiller-Flotten show B_q values below unity in the low to medium sensitive clay and values close to unity in the quick clay (Figure 14). Again, the values are fairly consistent between the various CPTU profiles.

The evaluation of soil type based on CPTU data can also be performed via empirical charts that assign a soil behavioural type (SBT), such as those presented by e.g. Robertson [30] and Schneider et al. [31]. Despite the widespread use of these SBT charts, the proper identification of sensitive and structured clays is not always so successful. Figure 15 presents the traditional soil behaviour type chart (SBT) from Robertson [30]. This system is based on the normalized cone resistance parameter

Q_t and the normalized friction ratio F_r, and on Q_t and B_q. Both charts on Figure 15 manage to distinguish between the low sensitivity and sensitive clay units. However, a significant portion of the quick clay data also falls in Zone 3 (clay to silty clay), 4 (silt mixtures) and 5 (sandy silt to clayey silt). Also, on these charts, the dry crust of Unit I classifies as a transitional silt and sand mixture.

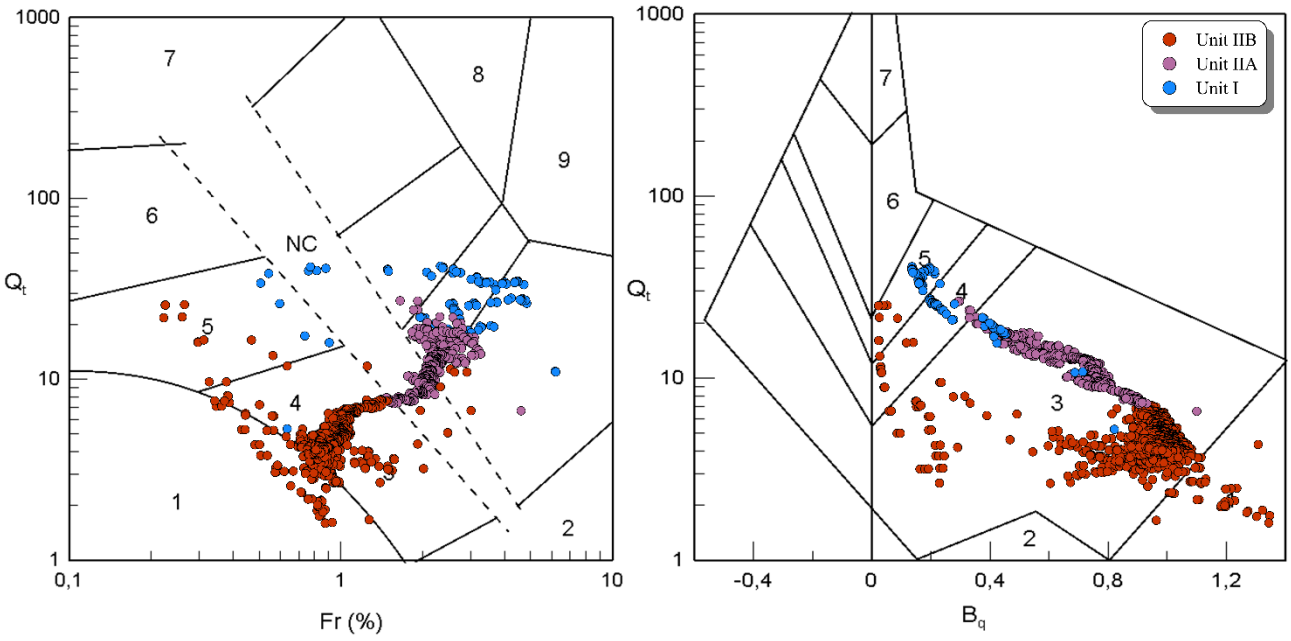

Figure 15. Robertson [30] soil behavior type chart for CPTU data (TILC01) on Tiller-Flotten clay. 1—Sensitive fine grained, 2—Clay–organic soil, 3—Clay–clay to silty clay, 4—Silt mixture, 5—Sand mixtures, 7—Dense sands, 8—Stiff sand to clayey sand (OC or cemented), 9—Stiff fine grained (OC or cemented).

5.7. Identification of quick clay from resistivity measurements

The use of geophysical methods such as electrical resistivity measurement is gaining popularity in Scandinavia and Canada for the identification of leached and potentially sensitive clay deposits e.g. [32,33]. It has been shown by a number of researchers that the measured electrical resistivity is strongly influenced by the salt content of the pore fluid, hence such method is useful to determine whether a clay deposit has been leached and has the potential of being sensitive. Solberg et al. [34] proposed the following scale of resistivity values for interpretation in clay deposits:

- Non-leached marine clay: 1–10 Ωm
- Leached, possibly quick clay: 10–80 Ωm
- Dry crust clay, slide deposits, coarser material like sand and gravel and bedrock: >80 Ωm

A total of six Electrical Resistivity Tomography (ERT) profiles were performed in November 2017 at the Tiller-Flotten site to map the extent of the clay deposit and to assess the leaching at the site. An example of two ERT profile acquisition is presented in Figure 16. The final RMS (root mean square of the misfit between the data and the models) is 0.7%, which is considered good. On all ERT profiles, the top 1–5 meters is marked by a resistive layer ($\rho > 100$ Ωm). This top layer corresponds

to the dry crust (Unit I) in the north and to a combination of the dry crust and overlying peat in the south where the resistive depth interval is thickest. Below the dry crust the ERT results are fairly constant with values ranging from 30 to 40 Ωm down to about 35 m below ground level (i.e. elevation 90 m.a.s.l.). As seen here the ERT data cannot distinguish between the low and high sensitive clay of Unit II. In this case it seems that the whole clay deposit has been leached. However, an overleaching process could explain the low sensitivity of Unit IIa (cf. [35]). The ERT data at greater depth shows the presence of a more conductive layer with resistivity less than 10 Ωm. This could indicate that the clay at greater depth has not yet been leached.

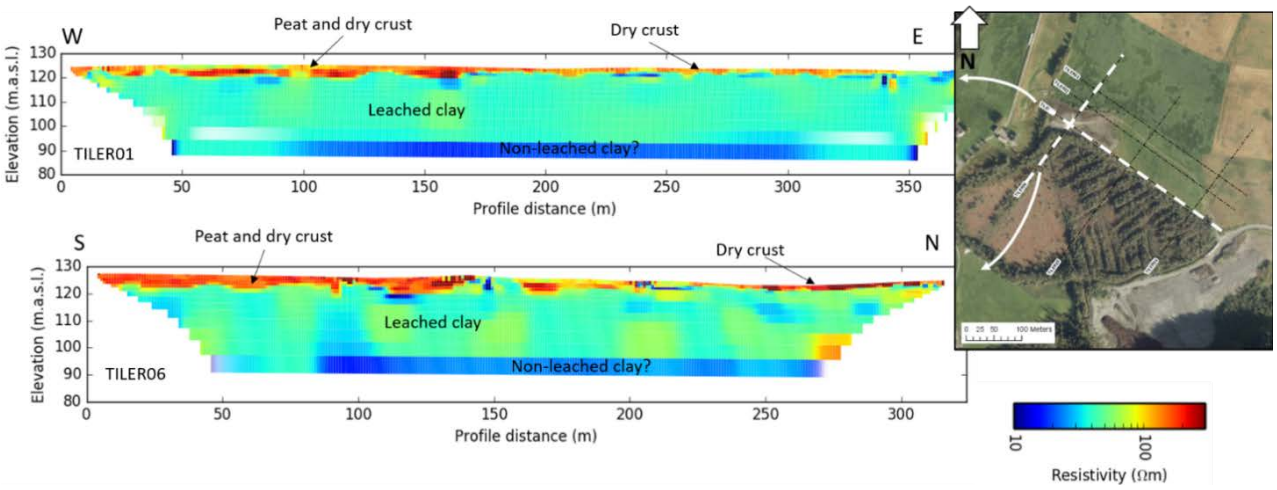

Figure 16. Typical results of electrical resistivity tomography at Tiller-Flotten.

Efforts have also been made to assess the reliability of the ERT results at Tiller-Flotten. Piezocone tests with a resistivity probe (RCPTU) were performed along some of the ERT profiles. A comparison of ERT and RCPTU data is shown in Figure 14. As can be seen on this figure the results are for all practical purposes very similar.

6. Engineering properties

6.1. Yield stress (or apparent preconsolidation stress)

Yield stress, or preconsolidation stress, have been estimated from 1D CRS oedometer test results (Figure 4). The results suggest that the preconsolidation stress is nearly twice the in situ vertical effective stress with an overconsolidation ratio (OCR) of 2.3 at a depth of 7 m and OCR value of 1.7 at 19.5 m. As discussed in chapter 4.4 the apparent overconsolidation of the clay is likely a result of the geological history in the area.

6.2. Overconsolidation ratio (OCR)

Overconsolidation ratio (OCR) values have been determined directly from oedometer test results using constant rate of strain (CRS) tests, and indirectly using results from dilatometer and

CPTU testing. For the oedometer tests, emphasis was given to high quality mini block samples collected between depths of 8.0 to 19.5 m. The OCR values are summarized on Figure 17 and can be seen to fall from above 5 near the surface to about 1.5 at 20 m depth.

Several authors have published relationships linking CPTU data to OCR (see [36]). For the Tiller-Flotten clay, the relationship proposed by Mayne [37] was used to assess OCR based on CPTU data. The Mayne [37] equation is given as follow:

$$OCR = k \cdot Q_t \tag{4}$$

where the empirical factor k is generally site specific and varying between 0.2–0.5. At Tiller-Flotten the best fit between Eq 4 and laboratory results is obtained using a *k* of 0.45 (Figure 17).

The OCR at Tiller-Flotten was also assessed using results from dilatometer tests (DMT) as shown on Figure 17. The original Marchetti [38] correlation for OCR in clay was used (i.e. OCR = $(0.5 \cdot K_D)^{1.56}$ where K_D is the horizontal stress index). Results seem for all practical purposes to fit well with both laboratory data and CPTU correlations.

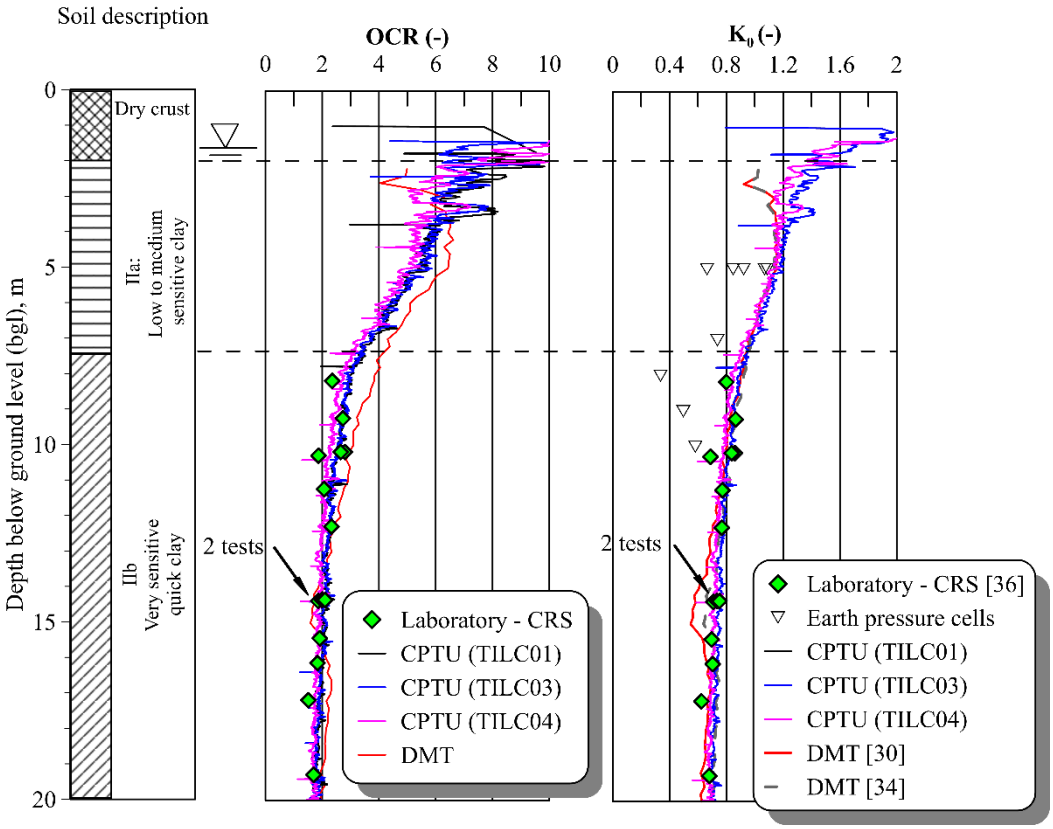

Figure 17. (Left) Overconsolidation ratio (OCR) and (right) coefficient of earth pressure at rest (K_0) with depth.

6.3. In situ horizontal stress

The coefficient of earth pressure at rest, K_0, is defined as the ratio of the effective horizontal stress σ'_H to the effective vertical stress σ'_V. The K_0-parameter is used in the design of, for example,

retaining walls, basement walls, pile foundations, pipelines and tunnels. It is also used for generating initial stresses when using advanced numerical methods to solve complex geo-engineering problems. The results of many types of laboratory tests also strongly depend on the estimate of K_0 (e.g. small strain shear modulus, G_{max}, from resonant column tests, strength and moduli from static and cyclic triaxial tests). Although K_0 can have a significant impact on inputs and calculation results, the reliability in the estimates of K_0 is still uncertain.

As seen from Figure 17, significant efforts have been made to determine K_0 at the Tiller-Flotten site using several tools and techniques. Results from DMT tests were evaluated using both the original Marchetti [38] equation and the equation proposed by Lacasse and Lunne [39] for estimation of K_0. The Marchetti equation was used with $\beta_k = 2$ as proposed by Hamouche et al. [40] for intact sensitive soils, while the Lacasse and Lunne equation was used with m = 0.64 for low plastic clays. Results show K_0 values decreasing from values close to 2.0 in the dry crust to values in the range 0.65–0.70 from 15 m below ground level and deeper.

Using laboratory and field data L'Heureux et al. [41] performed regression analyses and showed that for Norwegian clays the K_0 could be evaluated using the following equation:

$$K_0 = 0.53 \cdot OCR^{0.47} \tag{5}$$

This equation was used to estimate K_0 from OCR through laboratory data (i.e. CRS tests) and field data (i.e. CPTU) at Tiller-Flotten (Figure 17). Results are fairly consistent with that estimated from dilatometer data.

Push-in pressure cells were installed in the Tiller-Flotten clay to assess the horizontal stresses in the ground and evaluate K_0. At first, five different cells were installed at a depth of 5 m to assess the repeatability of the equipment. As seen on Figure 17, large scatter in K_0 was obtained. The reason for the unreliability of this tool may be attributed to the degree of disturbance during the installation, but also to the fragility of the tool that easily bend during the installation and thus measured stresses induced by bending moments. In general the push-in pressure cells gave lower K_0 values than that estimated by other techniques at the site.

6.4. Stiffness–Gmax

Shear wave velocity (V_s) data were obtained in situ by means of seismic dilatometer (SDMT), seismic cone penetration tests (SCPTU) and multichannel analysis of surface wave (MASW) at Tiller-Flotten. In the laboratory, V_s data were acquired using bender elements on high quality block prior to testing in the triaxial cell (i.e. unconfined state) ($V_{s,0}$) and inside the triaxial cell at in situ stresses ($V_{s,1}$).

The small strain stiffness is determined according to the elastic theory using the following equation:

$$G_{max} = \rho \cdot V_s^2 \tag{6}$$

where G_{max} is the small strain stiffness (in Pa), V_s is the shear wave velocity (in m/s), and ρ is the density (in kg/m^3). A comparison of all acquired V_s data and estimated G_{max} data is presented in Figure 18. As seen on this figure, the results obtained using the different in situ field techniques are

for all practical purposes very similar. The measured values show V_s to increase from approximately 120 m/s below the dry crust to 225 m/s at 20 m below ground level. These are characteristic values for Norwegian soft marine clays and are very similar to measured values for other sites in the Trondheim area [42,43].

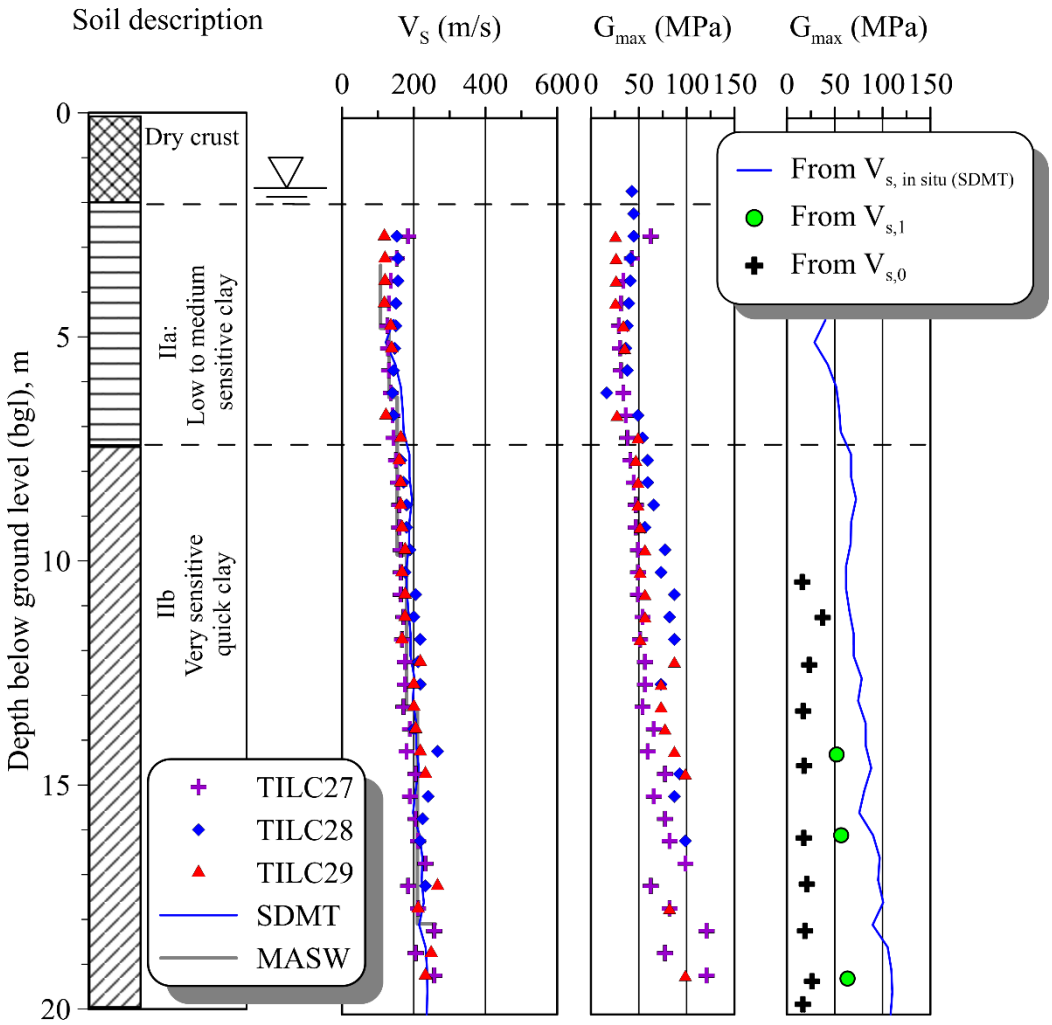

Figure 18. Shear wave velocity (V_s) and small strain shear modulus (G_{max}) with depth. MASW data from Olafdottir et al. [44].

G_{max} and V_s are primarily functions of soil density, void ratio, and effective stress, with secondary influences including soil type, age, depositional environment, cementation, and stress history c.f., Hardin and Drnevich [45]. Results from Tiller-Flotten show that $V_{s,0}$ and $V_{s,1}$ are consistently lower than those obtained in situ (Figure 18). This is attributed to both stress relief in the samples following sampling and to sample disturbance effects. Reconsolidation to in situ stresses (i.e. $V_{s,1}$) gave shear wave velocity values 20% less than in situ values. In terms of G_{max}, and according to Eq 6, this results in a percent change of ca. 44%.

6.5. Behavior in the oedometer tests

The classical Janbu [46] plot of 1D compression stiffness against stress is shown in Figure 19. The tangent modulus (or the constrained modulus) is defined as the ratio of the change of stress ($\Delta\sigma'$) to the change in strain ($\Delta\varepsilon$) for a particular load increment, i.e. $M = \Delta\sigma'/\Delta\varepsilon$. For a low stress level, around the in situ vertical effective stress (σ'_{v0}) the resistance against deformation (M_0) is large. Resistance reaches a minimum (M_L) around the preconsolidation stress (p'_c). Subsequently when the effective stress is increased beyond p'_c the resistance increases linearly with increasing effective stress.

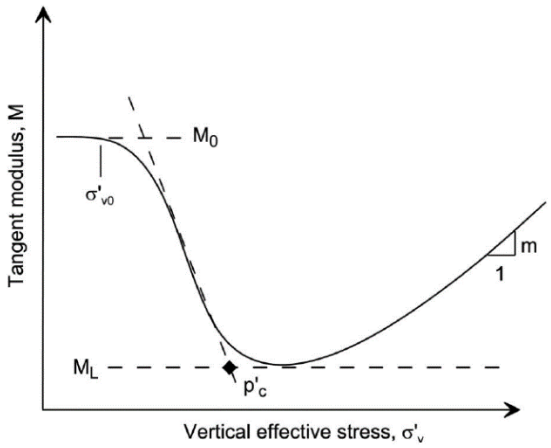

Figure 19. NGI interpretation of classical Janbu tangent modulus versus stress model.

A detailed description of equipment and procedures used at NGI for constant rate of strain (CRS) oedometer test is given by Sandbækken et al. [47]. Results from typical CRS tests on high quality block samples from the Tiller-Flotten site are presented in Figure 20. The results are presented in conventional log σ'_v versus axial strain (ε_a) format, as M versus σ'_v and also as coefficient of consolidation (c_v) versus σ'_v. The constrained modulus and the coefficient of consolidation is seen to be highest in the overconsolidated zone as expected. These values both drop sharply as the pre-consolidation (p'_c) pressure is approached and thereafter increase linearly with stress post p'_c. The slope of the M-σ'_v past p'_c is defined as the modulus number m (Figure 19).

The CRS test results presented in Figure 20 also include typical data from a test on a 54 mm piston sample for comparison with the high quality block samples. CRS results on the 54 mm piston sample show lower values of M and c_v before and near p'_c, a lower p'_c value and a higher modulus number m or stiffness in the normally consolidated zone.

Figure 21 presents values of M_0, M_L and m with depth as interpreted from CRS tests. In general the values of M_0 and M_L show an increase with depth, whereas the modulus number m is fairly constant. Estimates of M_0 and M_L based on in situ V_s data and on Eqs 7 and 8 proposed by L'Heureux and Long [42] are compared to laboratory results in Figure 21. The comparison is for all practical purposes very similar, and an increase in difference with depth is likely linked to sample disturbance effects.

$$M_0 = 0.0001 \cdot V_s^{2.212} \tag{7}$$

$$M_L = 0.00000014 \cdot V_s^{3.26} \tag{8}$$

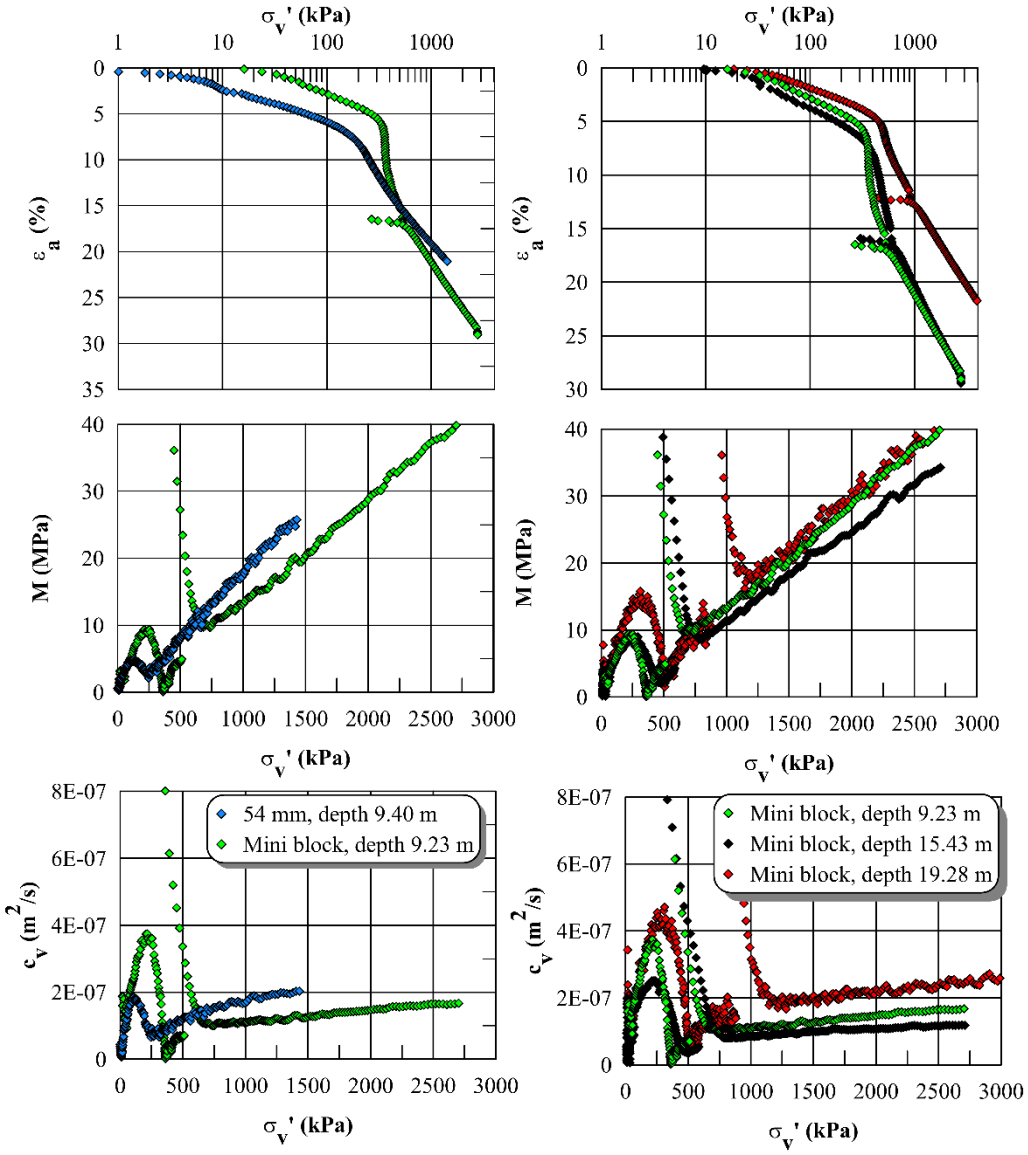

Figure 20. Typical CRS oedometer test results. (Left) Comparison of tests performed on a high quality mini-block sample and on a 54 mm piston sample. (Right) Comparison of CRS results obtained from mini-block samples at 9.23 m, 15.43 m and 19.28 m.

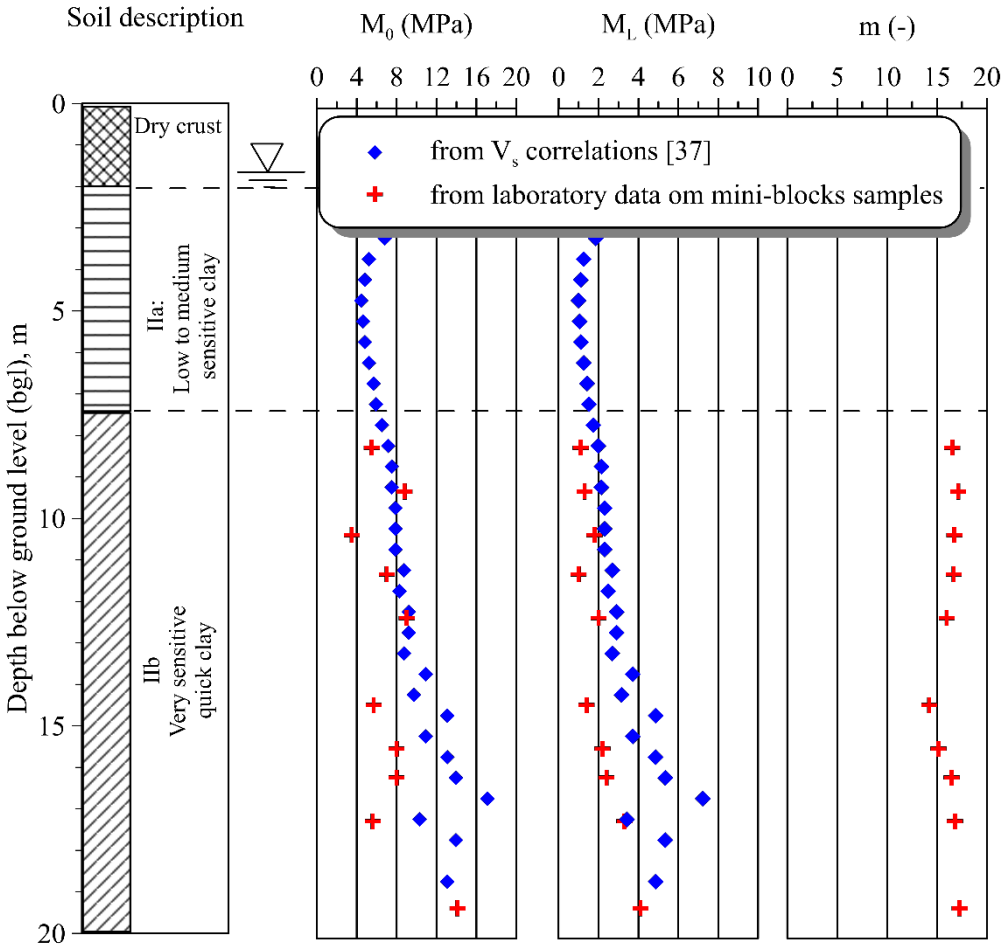

Figure 21. Plots of M_0 (constrained modulus at σ'_0), M_L (constrained modulus at σ'_p) and modulus number m versus depth.

6.6. Permeability coefficient and coefficient of consolidation

Permeability coefficient (k) values derived from CRS oedometer tests are presented on Figure 22. These permeability values were determined at the in situ stress level σ'_0 in the CRS tests using the method presented by Sandbækken et al. [47]. The permeability at the in situ stress state in the sensitive clay unit are consistent and ranges from 5×10^{-10} to 1.5×10^{-9} m/s. These values are similar to those reported for other Norwegian clays e.g. [48,49].

For one-dimensional compression, the coefficient of consolidation (c_v) can be determined using the well-known relationship:

$$c_v = \frac{k \cdot M}{\gamma_w} \tag{9}$$

where k is the coefficient of permeability, M is the constrained modulus as defined above and γ_w is the unit weight of water. By using Eqs 7 and 9, and by assuming a constant value of k of 5×10^{-10} m/s one can obtain a first approximation of c_v with depth at Tiller-Flotten using the in situ V_s results (Figure 22). These results are for all practical purposes similar to values of c_v determined at σ'_0 ($c_{v,\sigma'0}$)

using oedometer CRS tests (Figure 22). In general, the c_v values show a slight increase with depth with an average value of 11 m^2/yr.

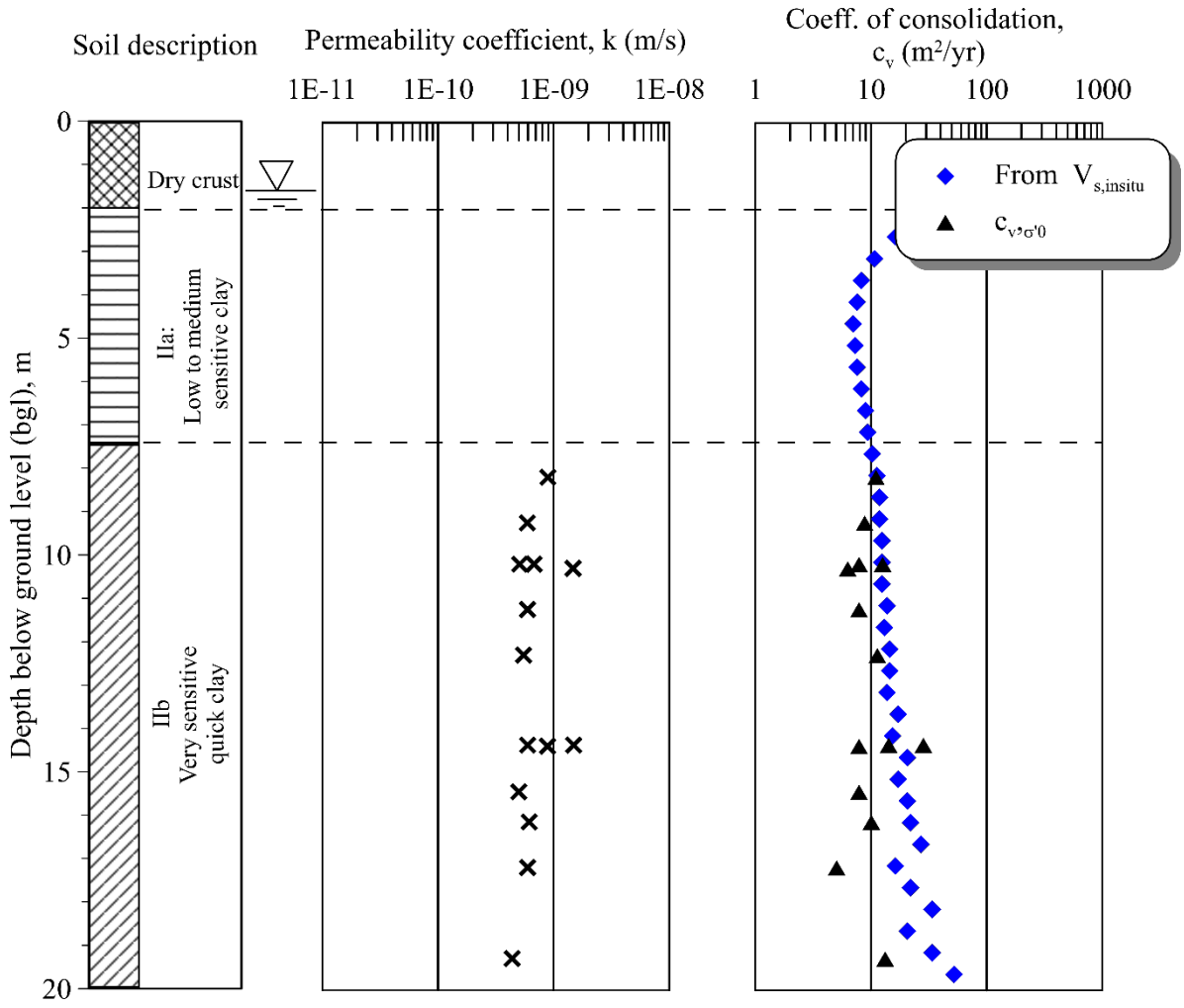

Figure 22. Permeability coefficient (k) and coefficient of consolidation (cv, σ'0) with depth.

6.7. Undrained shear strength

The undrained shear strength of a clay is commonly adopted in limit equilibrium analyses when the rate of loading is much greater than the rate at which pore water pressures may dissipate. For a given clay, the undrained shear strength depends on a number of factors such as e.g.: i) rate of loading, ii) stress path and iii) stress orientation. In general this means that the strength obtained from different tests at a given depth in a clay may give different results c.f. [50,51]. For this purpose, the clay at Tiller-Flotten has been investigated using different methods both in situ and in the laboratory.

In the laboratory the undrained shear strength of the Tiller-Flotten clay was evaluated by means of anisotropically consolidated undrained compression tests (CAUC) and anisotropically consolidated undrained extension tests (CAUE). For both type of tests, the best estimate of in situ stresses shown in Figure 4 was used for consolidation with K_0 derived from Eq 5 and Figure 17.

Stress path results from both (CAUC) and (CAUE) tests are presented in Figure 23. Similarly typical results from CAUC tests are presented in Figure 24 on a stress-strain diagram and a pore pressure plot. All tests show that the quick clay samples from Unit IIB behave in a contractive strain-softening manner. Samples from all depths tested show a pronounced peak at a strain of about 1%. The observed loop past the critical state line on the CAUC stress path plots confirm that the samples are structured.

All CAUC and CAUE tests presented in Figures 23 and 24 were carried out on either mini block samples or large diameter block samples on the clay from Unit IIB. As seen in Figure 24, results obtained from both sampler types are for all practical purposes identical. However, when comparing with smaller diameter samples, such as 72 mm, differences up to 45% in peak strength are observed (Figure 24).

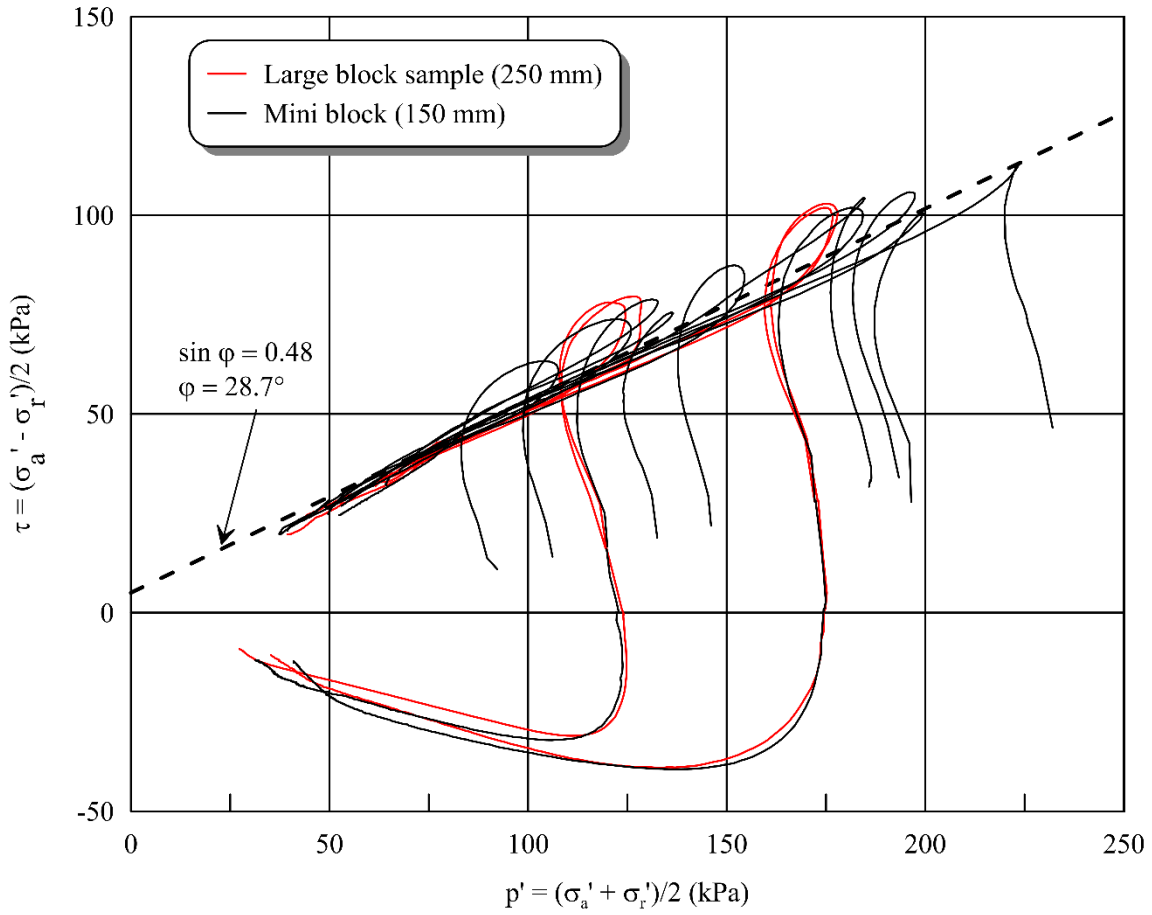

Figure 23. Triaxial stress/strain paths from CAUC and CAUE tests on mini block samples and large diameter block samples from Unit IIB.

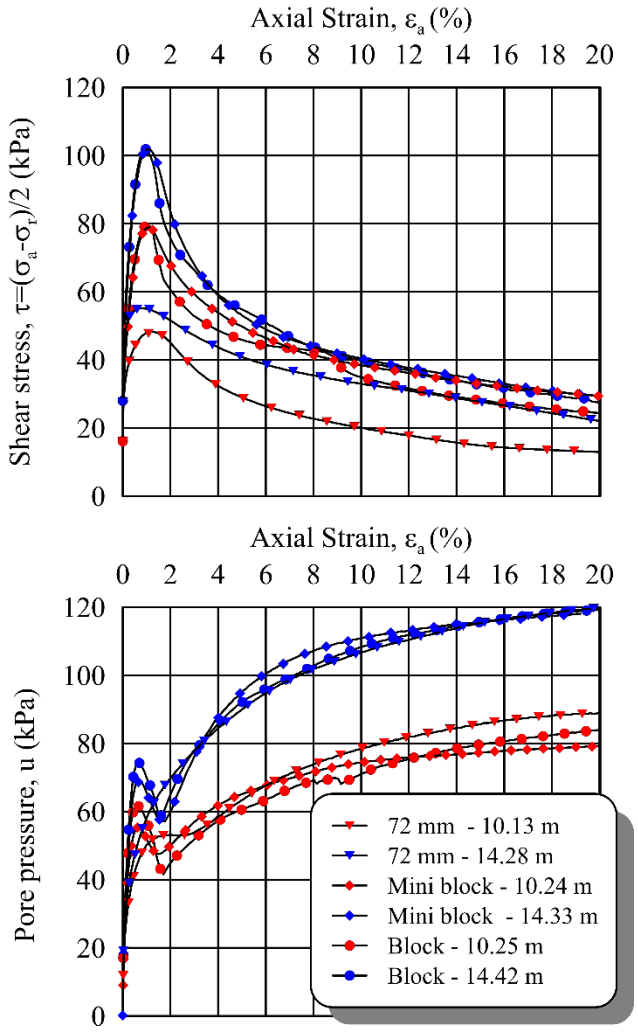

Figure 24. Typical CAUC triaxial test results from samples at two different depths and collected using a 72 mm piston sampler, a mini-block (150 mm) sampler and the Sherbrooke block sampler (250 mm).

In the laboratory, the undrained shear strength was also evaluated by means of index testing that included unconfined compression tests ($s_{u,UC}$) and fall cone tests ($s_{u,FC}$). Results from all index tests and the more advanced tests are presented on Figure 25. Of all methods, the fall cone tests conducted on the 54 mm samples clearly give the lowest undrained shear strength values. Above ca. 7 m (i.e. in Units I and IIa), $s_{u,FC}$ values are relatively high, between 20 kPa and 80 kPa, probably reflecting the higher degree of overconsolidation in this zone. Minimum $s_{u,FC}$ values are recorded towards the top of the quick clay zone. Then, the $s_{u,FC}$ values increase gradually with depth but fall well below the s_u/σ'_0 = 0.2–0.3 envelope, which corresponds to a normally consolidated material [52]. The reason for this is likely due to the combined effects of sample disturbance and the fact that the laboratory tests are carried out without a confining stress. The $s_{u,FC}$ obtained from tests on block samples are closer to the normally consolidated envelope due to higher sample quality, but values are still low compared to other methods. Results from unconfined compression tests are generally more consistent then fall cone data and generally plot within or close to the s_u/σ'_0 = 0.2–0.3 range.

Results from CAUC, CAUE and DSS tests against depth are also shown in Figure 25. The classical relationship with $s_{u, CAUC}$ greater than $s_{u, DSS}$, which is in turn is greater than $s_{u, CAUE}$, is seen to apply. Normalised shear strength data (s_u/σ'_{v0}) is also shown on Figure 25. The $s_{u, CAUE}$ values increase linearly with depth, from a value of 60 kPa at 7.5 m below ground level to a value of 110 kPa at a depth of 19 m. The normalized undrained shear strength ratio obtained from CAUC tests range from 0.40 to 0.61 in the very sensitive clay of Unit IIB (Figure 25).

One measure of the anisotropic nature of clay is determined by the anisotropic strength ratio:

$$K_1 = \frac{s_{u,CAUE}}{s_{u,CAUC}} \tag{10}$$

$$K_2 = \frac{s_{u,DSS}}{s_{u,CAUC}} \tag{11}$$

The anisotropic strength ratio are fairly constant in the quick clay of Unit IIB with K_1 ranging from 0.38 to 0.41 and K_2 ranging from 0.47 to 0.51. These values are lower and higher than those recommended in Norwegian practice [53], respectively. However, the K_1 value is equivalent to that suggested by Ladd [54] for lightly to normally consolidated clays and following a relationship of the form:

$$K_1 = 0.37 + 0.0072 I_p \tag{12}$$

Ladd and Foott [52] proposed that s_u be expressed in a normalised form (s_u/σ'_{v0}) in relation to the overconsolidation ratio (OCR) as follows:

$$\frac{s_u}{\sigma'_{v0}} = \alpha \cdot OCR^m \tag{13}$$

where σ'_{v0} is the present overburden pressure (in kPa) and α and m are curve fitting parameters. This principle, also called the SHANSEP approach, is often used in practice for assessing s_u based on the history of a clay deposit. The best-fit values of α and m based on a limited number of tests at Tiller-Flotten indicate good agreement with the average values found by Karlsrud and Hernandez-Martinez [49] for $s_{u, CAUC}$ (α = 0.31 and m = 0.70 at Tiller-Flotten) and $s_{u, CAUE}$ (α = 0.12 and m = 0.80 at Tiller-Flotten). However, the α and m values for $s_{u, DSS}$ (α = 0.16 and m = 0.75 at Tiller-Flotten) tend to fit better with the proposed lower range by [49].

As seen on Figure 25, the undrained shear strength at Tiller-Flotten was also investigated in situ by means of CPTU, FVT and DMT methods. The undrained shear strength from CPTU data was assessed using the SHANSEP approach i.e. Eq 13, and by first calculating OCR using Eq 4. Results fit remarkably well with data obtained from CAUC tests in the laboratory (Figure 25).

The uncorrected field vane test (FVT) yields quite low undrained shear strengths (Figure 25). It falls far below the DSS and CAUE strength. This could be attributed to soil strength anisotropy (Flaate [55]) combined with the low plasticity index of the clay (Soydemir [56]). Other factors such as vane insertion disturbance effects and failure mode (Gylland et al. [57]) could also have played a role.

The DMT data was evaluated using the original Marchetti equation [38]. Strength values from DMT are close to CAUC strength and to the lower bond of the CPTU data in Figure 25. However,

the DMT data shows a distinct decrease in strength at approximately 15 m depth, while no other test methods indicate such behavior. The reason for this is still unclear at this stage.

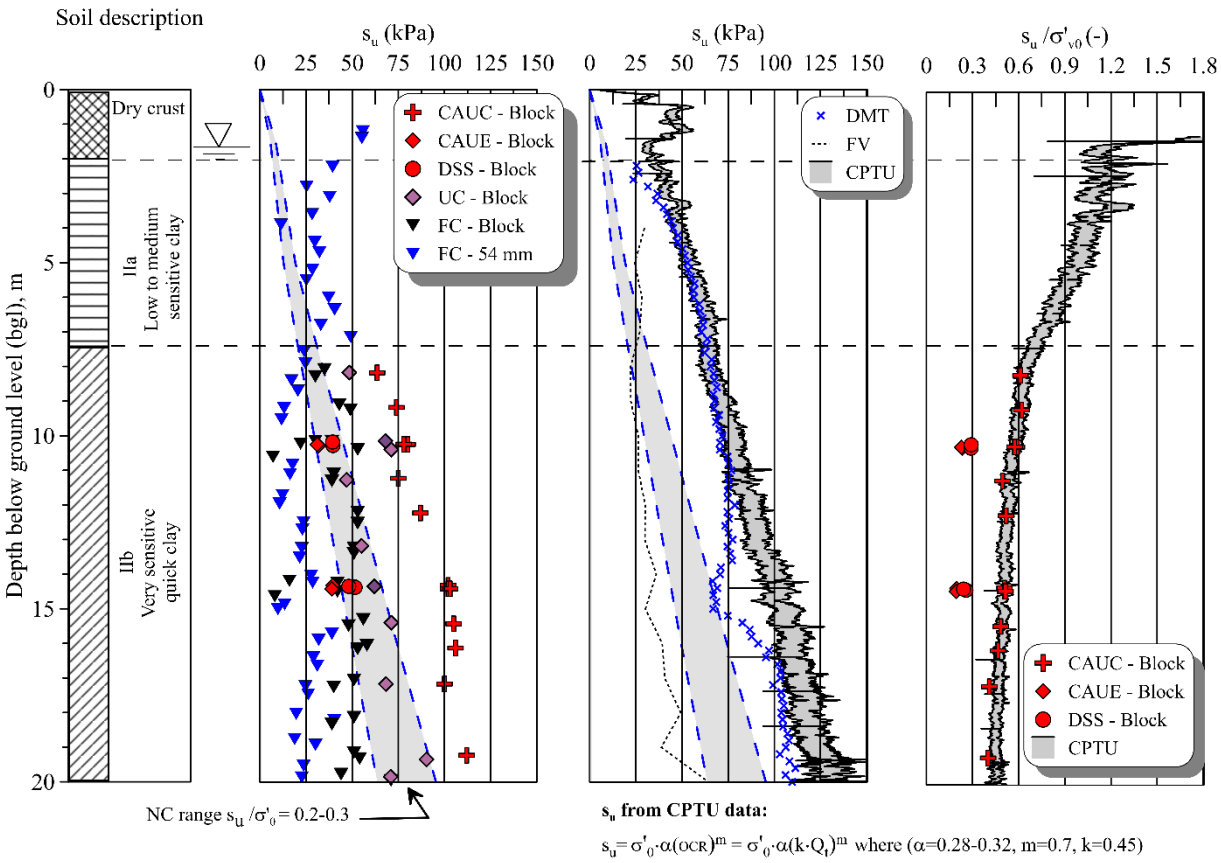

Figure 25. Undrained shear strength and undrained shear strength ratio with depth from laboratory and in situ field tests at Tiller-Flotten.

6.8. Drained shear strength

CAUC triaxial tests presented on Figure 23 suggest that the Tiller-Flotten clay has an effective friction angle (φ') in the range 29–32° with a small cohesion intercept (c') of about 5 kPa.

7. Discussion on quality and reliability of data

The quality and reliability of laboratory and field test data in sensitive clay can significantly be affected by sample disturbance. In turn, sample disturbance may affect key design parameters such as compressibility, preconsolidation stress (Figure 20) and undrained shear strength (Figure 24). Hence high quality data is a prerequisite if the geotechnical profession aims to improve geotechnical design, make it cost effective, and to reduce risks related to e.g. landslides and foundation failures in sensitive clays.

Methods developed to assess the quality of clay samples have existed for over two decades. Lunne et al. [58] proposed a method based on the normalized change in void ratio, $\Delta e/e_0$, evaluated

during the recompression of the sample to its in situ effective stress. The later is used to evaluate sample quality both in the triaxial cell and in the oedometer cell. Karlsrud and Hernandez-Martinez [49] proposed a method comparing the constrained modulus at in situ stress (M_0) and at σ'_p (M_L) to assess sample quality from oedometer test results. For a quick assessment of sample quality other authors have suggested to measure V_s immediately after removal from the subsurface on unconfined samples [59–61]. Simultaneous measurements of soil suction (u_r) measurements, enabling differences between unconfined and in situ stress state to be taken into account, have also been suggested [59,60,62,63].

A sample quality assessment based on the above methods and including i) M_0/M_L ratio [49], ii) $\Delta e/e_0$ [58], iii) $V_{s\text{-}lab}/V_{s\text{-}field}$ [59,63] and iv) u_r/σ'_{v0} [61,62] is presented on Figure 26. The sample quality assessment is conducted on the mini-block (φ = 160 mm) and block samples (φ = 250 mm) collected at the site. In general, the methods based on M_0/M_L, $V_{s\text{-}lab}/V_{s\text{-}field}$, u_r/σ'_{v0} classify the samples as either "very good to excellent" or "good to fair". A similar conclusion can be drawn from the $\Delta e/e_0$ evaluation performed on CAUC triaxial tests. However, the $\Delta e/e_0$ criterion applied to CRS test results suggest a poor quality for several of the samples. The reason for this is not believe to be linked with the quality of the samples, but rather with the way the CRS tests are carried in the laboratory. In fact, one clearly sees that the large diameter samples have retained their structure following sampling when looking at the CRS test results (Figure 20). It is easy to identify σ'_p for all of the block tests using both the σ'_v/ε and the σ'_v/M plots. The constrained modulus at in situ stress M_0 and M_L are also well defined as is the modulus number (m).

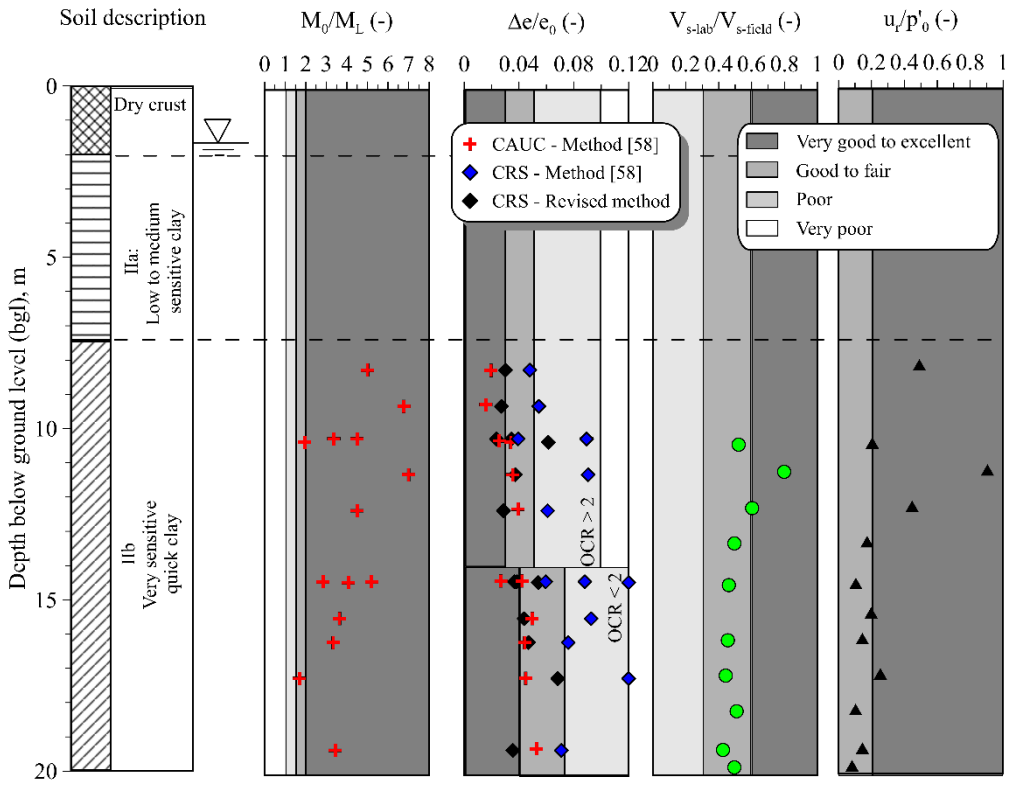

Figure 26. Evaluation of sample quality based on i) M_0/M_L ratio [49], ii) $\Delta e/e_0$ [58], iii) $V_{s\text{-}lab}/V_{s\text{-}field}$ [59,63] and iv) u_r/σ'_{v0} [61,62].

The large axial strain measured in the oedometer cell up to p'_0 on the sensitive Tiller clay may be attributed to contact being made with the sample, rather than sample quality. Much of the axial strain in this region seems to be due to false deformations. The reason could be attributed to a thin zone of remoulded, very compressible, material that forms at all boundaries of the specimen during sample preparation. For oedometer specimens, which are cut out by a cutting cylinder, this also gives false radial strain, and more so the more sensitive the material is.

A look at CRS data from Tiller-Flotten indicate that that the false deformation can be corrected for by extending a tangent line to the stress strain curve, starting from p_o', upwards until it intersects the strain axis (Figure 27). According to Berre and Lunne (pers. comm.) the intersection point can be used to define the amount of false deformation which should be excluded in the strain used to determine, $\Delta e/e_o$. This implies that the tangent modulus, M, is assumed to be constant, at least up to p_o'. This assumption is similar to the ideas brought by Janbu [46]. The sketch on Figure 27 indicates how the correction can be made to evaluate sample quality based on the $\Delta e/e_0$ criterion on the sensitive Tiller clay.

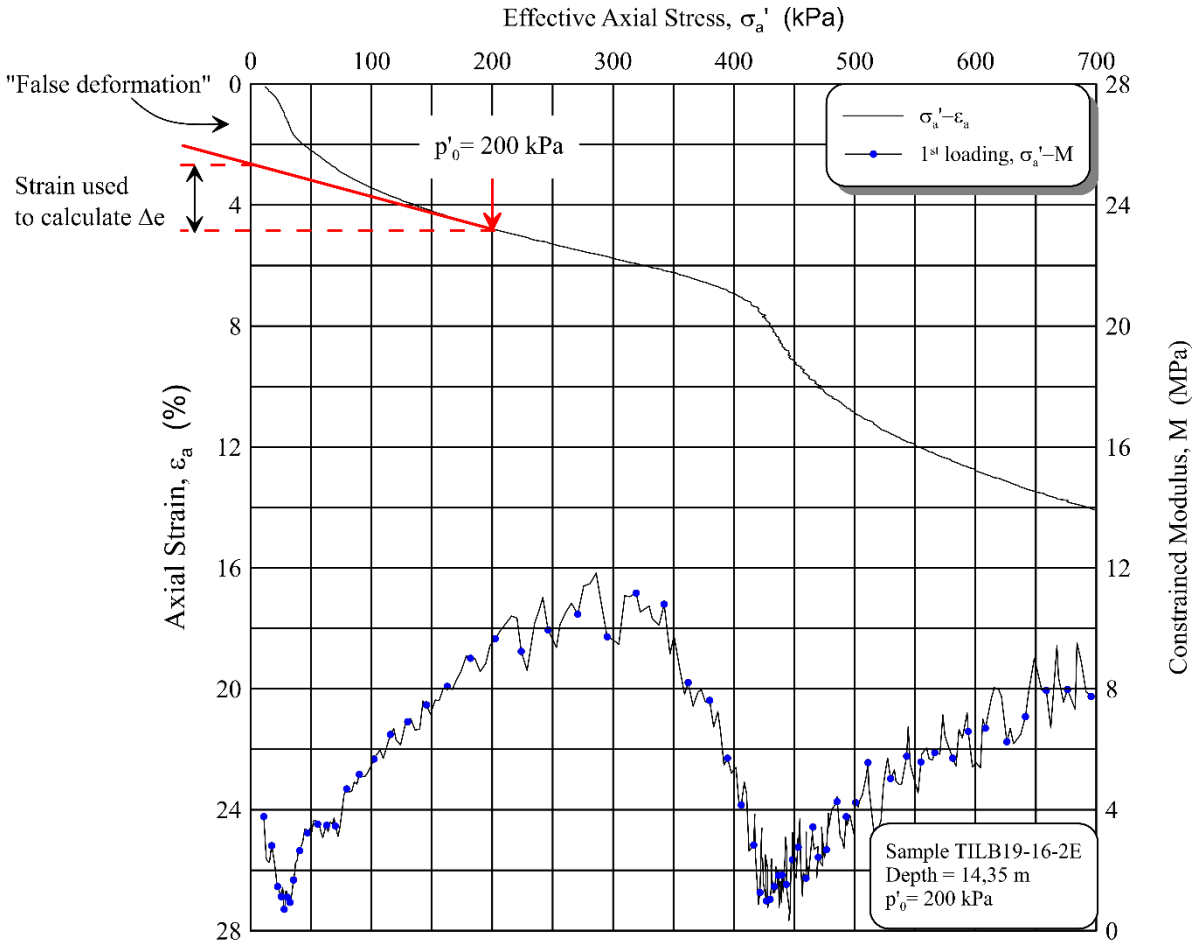

Figure 27. Proposed method to determine Δe for sample quality evaluation using the $\Delta e/e_0$ criterion and results from CRS oedometer test carried out on the sensitive clays (Berre and Lunne, pers. comm).

Sample quality for all the CRS oedometer test results from Tiller-Flotten was re-evaluated using the normalized change in void ratio method with the correction described above. As anticipated, results shown on Figure 26 give a much higher sample quality when neglecting false deformation. The results also show better consistency with the $\Delta e/e_0$ sample quality evaluation conducted on the same block, but from CAUC test results. It is expected that the revised $\Delta e/e_0$ sample quality assessment method for CRS test results proposed herein and by Berre and Lunne (pers. comm.) will give similar results for other sensitive and quick clays. Nevertheless it should be tested on a range of clays with different sensitivities to better understanding when this correction should be used in practice.

8. Conclusion

This paper has detailed the characteristics and engineering properties of the Tiller-Flotten clay, a thick deposit of sensitive marine clay. A wide variety of laboratory tests, in situ tests and geophysical tests have been used to characterize the remarkably uniform clay deposit and to assess its engineering properties. The clay at Tiller-Flotten is slightly overconsolidated and shows a low to medium plasticity. From 7.5 m below the ground surface the clay shows a very high sensitivity and is classified as quick following the Norwegian standards. The properties of the Tiller-Flotten clay show good agreement with some well-known correlations. Sample disturbance effects are shown to have important impact on the measured properties of the material, such as compressibility, preconsolidation stress and undrained shear strength.

The Tiller-Flotten quick clay site is part of the Norwegian GeoTest Sites infrastructure and is available for the entire geotechnical community for basic and applied research and education on soil testing, soil behavior and calibration of design methods. The research infrastructure will contribute to increased outreach and greater cohesion of geotechnical data in Norway and abroad. It is hoped that the next years will see an increased use of this benchmark site as a research tool, and for training and teaching purposes. Information about the site will be shared with research organizations and the public through the project website (http://www.geotestsite.no/) designed for easy search and archiving capability.

Acknowledgements

The authors wish to thank The Research Council of Norway for their generous infrastructure grant to establish the Norwegian GeoTest Sites infrastructure (NGTS) (Grant No. 245650/F50). A special thanks to Prof. Ariane Locat and Dr. Ana Priscilla Paniagua Lopez for reviewing the manuscript and providing constructive comments. The authors would also like to acknowledge the valuable inputs from Tom Lunne and Toralv Berre on chapter 7. Finally, the authors are grateful to a large number of colleagues at NGI and NTNU who have contributed significantly to the work presented in this paper.

Conflict of interest

All authors declare no conflicts of interest in this paper.

References

1. Gregersen O (1981) The quick clay landslide in Rissa, Norway. *Nor Geotech Inst Publ* 135: 1–6.
2. L'Heureux JS, Eilertsen RS, Glimsdal S, et al. (2012) The 1978 quick clay landslide at Rissa, mid Norway: subaqueous morphology and tsunami simulations. *Submarine mass movements and their consequences*, Springer, 507–516.
3. Lacasse S (2013) 8th Terzaghi Oration Protecting society from landslides–the role of the geotechnical engineer, 15–34.
4. Solberg IL, Long M, Baranwal VC, et al. (2016) Geophysical and geotechnical studies of geology and sediment properties at a quick-clay landslide site at Esp, Trondheim, Norway. *Eng Geol* 208: 214–230.
5. L'Heureux JS, Lunne T, Lacasse S, et al. (2017) Norway's National GeoTest Site Research Infrastructure (NGTS). Unearth the Future, Connect beyond Proceedings of the 19th International Conference on Soil Mechanics and Geotechnical Engineering.
6. Gylland A, Long M, Emdal A, et al. (2013) Characterisation and engineering properties of Tiller clay. *Eng Geol* 164: 86–100.
7. Leroueil S, Hamouche K, Ravenasi F, et al. (2003) Geotechnical characterization and properties of a sensitive clay from Quebec. In: Tan TS, Phoon KK, Hight DW, et al., *Characterisation and engineering properties of natural soils*, 1: 363–394.
8. Reite AJ, Sveian H, Erichsen E (1999) *Trondheim fra istid til nåtid: landskapshistorie og løsmasser*. Norges geologiske undersøkelse.
9. Long M, L'Heureux JS, Fiskvik Bache BK, et al. (2019) Site characterisation and example of results from large scale testing at the Klett quick clay research site. *AIMS Geosci* 5: 344–389.
10. Quinteros S, Gundersen A, L'Heureux JS, et al. (2019) Øysand research site: Geotechnical characterization of deltaic sandy-silty soils. *AIMS Geosci* 5: 750–783.
11. L'Heureux J, Carroll R, Lacasse S, et al. (2017) New Research Benchmark Test Sites in Norway. *Geotech Front 2017*, 631–640.
12. NGI (2016) Standardization of in situ tests and field work. Oslo, Norway: Norwegian Geotechnical Institute (NGI), 37.
13. NGI (2016) Laboratory procedures and standards for the NGTS project. Oslo, Norway: Norwegian Geotechnical Institute (NGI), 45.
14. Emdal A, Gylland A, Amundsen HA, et al. (2016) Mini-block sampler. *Can Geotech J* 53: 1235–1245.
15. undersøkelse Ng, Misund A, Banks D, et al. (1994) *Weichselian and Holocene geology of Sør-Trøndelag and adjacent parts of Nord-Trøndelag county, Central Norway*, Norges geologiske undersøkelse.
16. Reite AJ (1995) Deglaciation of the Trondheimsfjord area, central Norway. *Norg Geol Unders Bull* 427: 19–21.

17. Andersen BG, Mangerud J, Sørensen R, et al. (1995) Younger Dryas ice-marginal deposits in Norway. *Quat Int* 28: 147–169.
18. Wolff FC (1979) *Beskrivelse til de berggrunnsgeologiske kart Trondheim og Østersund, 1: 250, 000*. (In Norwegian). Norges geologiske undersøkelse (NGU), 55.
19. Rosenqvist IT (1953) Considerations on the sensitivity of Norwegian quick-clays. *Geotechnique* 3: 195–200.
20. Bjerrum L (1973) Problems of soil mechanics and construction on soft clays and structurally unstable soils, Proc. 8th ICSMFE, 111–159.
21. Bjerrum L (1967) Engineering geology of Norwegian normally-consolidated marine clays as related to settlements of buildings. *Geotechnique* 17: 83–118.
22. Moum J (1965) Falling drop used for grain-size analysis of fine-grained materials. *Sedimentology* 5: 343–347.
23. NGF (2011) Veiledning for symboler og definisjoner i geoteknikk: Identifisering og klassifisering i jord. Norwegian Geotechnical Society Oslo, Norway.
24. Mitchell JK, Soga K (2005) Fundamentals of soil behavior. *Fundamentals of soil behavior*. NJ: John Wiley & Sons.
25. Leroueil S, Tavenas F, Samson L, et al. (1983) Preconsolidation pressure of Champlain clays. Part II. Laboratory determination. *Can Geotech J* 20: 803–816.
26. Burland JB (1990) On the compressibility and shear strength of natural clays. *Géotechnique* 40: 329–378.
27. Gylland AS, Rueslåtten H, Jostad HP, et al. (2013) Microstructural observations of shear zones in sensitive clay. *Eng Geol* 163: 75–88.
28. NGF (1989) Veiledning for utførelse av dreiesondering.
29. Sandven R, Watn A (1995) Soil classification and parameter evaluation from piezocone tests: Results from the major site investigations at Oslo Main Airport, Gardermoen. *Proceedings of CPT'95* 3: 35–55.
30. Robertson PK (1990) Soil classification using the cone penetration test. *Can Geotech J* 27: 151–158.
31. Schneider J, Hotstream J, Mayne PW, et al. (2012) Comparing CPTU Q-F and Q-Δ u 2/σv0′ soil classification charts. *Géotech Lett* 2: 209–215.
32. Donohue S, Long M, L'Heureux JS, et al. (2014) The use of geophysics for sensitive clay investigations. *Landslides in Sensitive Clays*, Springer, 159–178.
33. Long M, Donohue S, L'Heureux JS, et al. (2012) Relationship between electrical resistivity and basic geotechnical parameters for marine clays. *Can Geotech J* 49: 1158–1168.
34. Solberg IL, Rønning JS, Dalsegg E, et al. (2008) Resistivity measurements as a tool for outlining quick-clay extent and valley-fill stratigraphy: a feasibility study from Buvika, central Norway. *Can Geotech J* 45: 210–225.
35. Helle TE, Nordal S, Aagaard P, et al. (2015) Long-term effect of potassium chloride treatment on improving the soil behavior of highly sensitive clay—Ulvensplitten, Norway. *Can Geotech J* 53: 410–422.
36. Priscilla P, D'Ignazio M, L'Heureux JS, et al. (2019) CPTU correlations for Norwegian clays: an update. *AIMS Geosci* 5: 82–103.

37. Mayne PW (1986) CPT indexing of in situ OCR in clays, ASCE, 780–793.
38. Marchetti S (1980) In situ tests by flat dilatometer. *J Geotech Geoenviron Eng* 106.
39. Lacasse S, Lunne T (1989) Calibration of dilatometer correlations. *Nor Geotech Inst Publ* 106: 299–321.
40. Hamouche KK, Leroueil S, Roy M, et al. (1995) In situ evaluation of K_0 in eastern Canada clays. *Can Geotech J* 32: 677–688.
41. L'Heureux JS, Ozkul Z, Lacasse S, et al. (2017) A revised look at the coefficient of earth pressure at rest for Norwegian Clays. In (NGF) NGS, Oslo, Norway.
42. L'Heureux JS, Long M (2017) Relationship between shear-wave velocity and geotechnical parameters for Norwegian clays. *J Geotech Geoenviron Eng* 143: 04017013.
43. Long M, Donohue S (2007) In situ shear wave velocity from multichannel analysis of surface waves (MASW) tests at eight Norwegian research sites. *Can Geotech J* 44: 533–544.
44. Olafsdottir EA, Bessason B, Erlingsson S, et al. (2019) Benchmarking of an open source MASW software using data from four Norwegian Geo-Test Sites, Proceedings of the XVII ECSMGE-2019.
45. Hardin BO, Drnevich VP (1972) Shear modulus and damping in soils: design equations and curves. *J Soil Mech Found Div* 98: 667–692.
46. Janbu N (1985) Soil models in offshore engineering. *Géotechnique* 35: 241–281.
47. Sandbækken G, Berre T, Lacasse S (1986) Oedometer testing at the Norwegian Geotechnical Institute. *Consolidation of soils: Testing and evaluation*, ASTM International.
48. Lunne T, Long M, Forsberg CF (2003) Characterisation and engineering properties of Onsøy clay. In: Tan TS, Phoon KK, Hight DW, et al., *Characterisation and engineering properties of natural soils*, 1: 395–427.
49. Karlsrud K, Hernandez-Martinez FG (2013) Strength and deformation properties of Norwegian clays from laboratory tests on high-quality block samples. *Can Geotech J* 50: 1273–1293.
50. Leroueil S, Hight DW (2003) Behaviour and properties of natural soils and soft rocks. In: Tan TS, Phoon KK, Hight DW, et al., *Characterisation and engineering properties of natural soils*, 1: 29–254.
51. Lacasse S, Jamiolkowski M, Lancellotta R, et al. (1981) In situ characteristics of two Norwegian clays, Proceedings of the 10th International Conference on Soil Mechanics and Foundation Engineering, 507–511.
52. Ladd CC, Foott R (1974) New design procedure for stability of soft clays. *J Geotech Geoenviron Eng* 100: 763–786.
53. Thakur V, Oset F, Viklund M, et al. (2014) En omforent anbefaling for bruk av anisotropifaktorer i prosjektering i norske leirer. *NVE, SV, JERNBANEVERKET (ed) Naturfareprosjektet Dp* 6.
54. Ladd CC (1991) Stability evaluation during staged construction. *J Geotech Eng* 117: 540–615.
55. Flaate K (1966) Factors influencing the results of vane tests. *Can Geotech J* 3: 18–31.
56. Soydemir C (1976) Strength anisotropy observed through simple shear tests. In Janbu N, Jørstad F, Kjærnsli B (Eds.), editor, *Laurits Bjerrum Memorial Volume—Contributions to Soil Mechanics Oslo, Norway*, Norwegian Geotechnical Institute (NGI), 99–103.

57. Gylland AS, Jostad HP, Nordal S, et al. (2013) Micro-level investigation of the in situ shear vane failure geometry in sensitive clay. *Geotechnique* 63: 1264.
58. Lunne T, Berre T, Strandvik S (1998) Sample disturbance effects in deep water soil investigations, Society of Underwater Technology.
59. Landon MM, DeGroot DJ, Sheahan TC (2007) Nondestructive sample quality assessment of a soft clay using shear wave velocity. *J Geotech Geoenviron Eng* 133: 424–432.
60. Hight DW, Leroueil S (2003) Characterisation of soils for engineering purposes. In: Tan TS, Phoon KK, Hight DW, et al., *Characterisation and engineering properties of natural soils*, 1: 255–360.
61. Tanaka H, SHARMA P, Tsuchida T, et al. (1996) Comparative study on sample quality using several types of samplers. *Soils Found* 36: 57–68.
62. Tanaka H, Nishida K (2007) Suction and Shear Wave Velocity Measurements for Assessing Sample Quality. *Stud Geotech Mech* 29: 163–175.
63. Donohue S, Long M (2010) Assessment of sample quality in soft clay using shear wave velocity and suction measurements. *Géotechnique* 60: 883–889.

Geosciences